3. Regional rainfall anomalies in Colombia and their association with ENSO: A phase synchronization approach

Hernán D. Salas, Germán Poveda, Óscar J. Mesa, and Jürgen Kurths

3.1. Abstract

We investigate Phase Synchronization (PS) between the El Niño - Southern Oscillation (ENSO) signal and the (inter-annual and annual) cycles of rainfall in Colombia. To that end, we carry out a detailed data analysis in order to define the annual cycle (AC), eliminating the seasonal residual frequencies in hydro-climatic anomalies (HyAns), assessing the statistical significance of PS metrics, and checking the sensitivity of the PS metrics in relation to diverse HyAns estimation methods. Then, we characterize the seasonal regional patterns of rainfall anomalies in relation to the ENSO's states. We find that the positive (negative) HyAns experienced in the Pacific, Caribbean and Andean regions of Colombia, during La Niña (El Niño), are phase-locked with the ENSO signal in the tropical Pacific Ocean, whereas the negative (positive) HyAns experienced in the Orinoco and Amazon regions, during La Niña (El Niño), do not show such phase-locking. Moreover, we provide evidence that the ENSO signal is phase-locked with the AC of rainfall in some regions of Colombia, which suggest that the AC plays an important role in the influence of ENSO on Colombian climatology and opens new paths towards the understanding of non-linear feedbacks between hydro-climatic processes. Our results show that, at inter-annual timescales, ENSO exhibits the strongest phase-locking with the annual and inter-annual cycles of rainfall throughout Colombia, although other macro-climatic processes also show significant PS such as the Pacific Decadal Oscillation (PDO) and the North Atlantic Oscillation (NAO). Moreover, we show that the highest positive (negative) rainfall anomalies over western Colombia coincide with the strong (weak) PS between the ENSO and the PDO signals. This work provides new evidence on the non-linear interactions between hydro-climatic processes in Colombia and

ENSO, and constitute an unexplored approach to the understanding of climatic anomalies in tropical South America.

3.2. Introduction

The hydro-climatic variability of Colombia is influenced by a suit of periodic and quasi-periodic processes acting on a wide range of time scales such as: the diurnal cycle of solar radiation and temperature (DC), tropical easterly waves (TEW), the Madden-Julian Oscillation (MJO), the annual cycle of solar radiation (AC), the Quasi-Biennal Oscillation (QBO), the El Niño-Southern Oscillation (ENSO), the Pacific Decadal Oscillation (PDO), the North-Atlantic Oscillation (NAO) and, the Atlantic Multidecadal Oscillation (AMO) [*Poveda and Mesa*(1997),*Poveda et al.*(2001),*Poveda et al.*(2002),*Poveda et al.*(2004),*Poveda et al.*(2005),*Poveda et al.*(2011)]. In this work, we aim to explore the non-linear interactions between the occurrence of ENSO over the tropical Pacific Ocean and the AC and rainfall anomalies (HyAns) in Colombia based upon the following arguments and observations.
First, there is a tendency in the scientific literature to disregard the importance of the annual cycle inherent in monthly the hydro-climate records, given that it explains the largest amount of variability. The AC is taken for granted and therefore most analysis are focused on the study of anomalies with respect to the annual cycle [*Wu et al.*(2008)]. Such an approach assumes that the hydro-climate variables have a constant response to the periodic incoming solar radiation (SR), disregarding the non-linear interactions of the Earth's climate system, while at the same time overlooking important interactions between the AC of hydro-climatic processes and other climatic processes at inter-annual timescales.
Second, in Chapter 2 was evidenced that HyAns can be defined through different methods, among them: *(i)* the Traditional Annual Cycle or constant climatology (HyAns–TAC), *(ii)* **F**-filtering of the Annual cycle by moving average (HyAns–FAC), *(iii)* Annual cycle extracted by Singular Spectrum Analysis (HyAns–SSAC) and, *(iv)* the Modulated Annual Cycle, which is based on the EEMD technique. Furthermore, the quantification of interdependence between climate time series during ENSO, at inter-annual timescales, can be biased due to: (i) the presence of a seasonal significant residual in time series of anomalies, (ii) the definition of constant or non-constant annual cycle, and (iii) the presence of high-frequencies (intra-annual variability and noise) in HyAns time series (see Chapter 2). Moreover, HyAns estimation techniques affect interdependence quantification, which leaves room for ambiguity in the physical interpretation of results (see Chapter 2). Hence, we point out the need to study the sensitivity of the linear and non-linear interdependence quantification techniques in relation to diverse HyAns methods.
Third, ENSO is one of the main controlling mechanisms of Earth's climate at inter-annual time scales. It is a conjoint process between *El Niño* (EN, oceanic component) and the *Southern Oscillation* (SO, atmospheric component). El Niño refers to the anomalous warming of the central and eastern waters of the tropical Pacific Ocean, which produces a deepening of

the oceanic's thermocline, concomitant with the weakening and (sometimes) reversal of the trade winds and the displacement of the core of convection from the western to the central and eastern regions of the tropical Pacific. The SO is a stationary wave that produces an atmospheric pressure see-saw between the western and eastern equatorial Pacific [*Sarachik and Cane*(2010)]. Recent works by [*Stein et al.*(2011), *Stein et al.*(2014)] have provided evidence of phase-locking between the AC of SSTs and the ENSO signal in the tropical Pacific Ocean using synchronization techniques. However, no study has used a similar approach to investigate the interrelations between ENSO and the AC of hydro-climatic variables in other regions. i.e northern South America. In particular, during the ENSO cold (warm) state, positive (negative) anomalies in rainfall and streamflows are experienced overall in Colombia, those causing extreme hydro-climatic events with important socio-economical, environmental and ecological impacts. Therefore, a better understanding of the influence of ENSO on Colombian hydro-climatic variability is fundamental to improve the diagnosis, modeling and forecasting of extreme hydro-climatic events [*Poveda and Mesa*(1997), *Poveda et al.*(2001), *Poveda et al.*(2011)].

Fourth, solar radiation (SR) is a periodic forcing on the Earth's non-linear climate system. In response to such periodic forcing the hydro-climatic variables contain a strong annual cycle (AC) signature which represents a high percentage of their variance. In the case of rainfall in Colombia, the AC exhibits an uni-modal and bi-modal behavior depending on the location in the country. For the most part, a bimodal annual cycle of rainfall is restricted to the Andean region of Colombia, while unimodality is witnessed off the Andes, with maximum rainfall associated with a shift of the ITCZ over Colombia [*Poveda et al.*(2015), *Urrea et al.*(2018)]. Bi-modality can be explained by the periodic forcing of the incoming SR which occurs twice each year, but uni-modality is observed also in areas where the periodic forcing of SR occurs twice each year. According to [*Hoyos et al.*(2017)], the Intertropical Convergence Zone (ITCZ) over the Orinoco and Amazon regions advances slower than over the rest of the country producing a unimodal convergence of moisture which contributes to explain the unimodaly in precipitation. Notwithstanding, physical processes involved in the AC of rainfall have not been satisfactory explained [*Urrea et al.*(2018)].

Finally, there is evidence of the interdependence between hydro-climatic variables of Colombia and the Pacific ocean-atmospheric dynamics at ENSO timescales [*Poveda et al.*(2001), *Waylen and Poveda*(2002), *Poveda et al.*(2011), *Bedoya-Soto and Poveda*(2017), *Bedoya-Soto et. al.*(2018)]. However, such interdependence has been studied by means of linear or non-linear statistical tools, while ignoring *the interaction between the oscillations* under the assumption that physical phenomena are generated by multiple oscillatory interacting systems or *synchronization* in the sense of [*Pikovsky et al.*(2001)]. Diverse types of synchronization are known, such as frequency synchronization (FS), phase synchronization (PS), identical synchronization (IS), generalized synchronization (GS) and lag synchronization (LS) [*Brown and Kocarev*(2000)]. In particular, for two oscillatory systems X and Y, PS (or phase-locking) means that the instantaneous phases of X, $\phi_x(t)$, are related to the instantaneous phases of Y, $\phi_y(t)$. If $|n_x\phi_x - m_y\phi_y| < c$, where n_x and m_y are natural integers, and c is a constant, both systems are in $n_x : m_y$ PS. In contrast, FS means a link between the frequencies such that if $|n_x\omega_x - m_y\omega_y| < c$, where n_x and m_y are natural integers and, c is a constant, both systems are in FS. Thereafter, PS implies FS but FS does not imply PS. In addition, the PS approach does not include either the interrelation between the amplitudes or control mechanisms such as Amplitude Modulation (AM), but the adequate characterization, quantification and explanation of the phases is valuable even if the amplitude interrelations are not well known [*Von Storch et al.*(1995)].

Hence, we aim to investigate the characteristics of PS between ENSO (system 1) and the (annual and inter-annual) cycles of rainfall in Colombia (system 2). Our goal is to characterize and quantify temporal and spatial PS patterns between both systems during La Niña and El Niño. Hypothetically, we consider that ENSO is the driver system and that rainfall in Colombia is the response system (the influenced system). To those ends, we use a set of non-linear and non-stationary data analysis techniques such as Ensemble Empirical Mode Decomposition (EEMD), Generalized Phase Difference (GPD), diverse HyAns estimation methods and an index that provides a measure of the strength of phase synchronization (SPS) between both systems. The existence of a phase relation implies the possibility to predict the phases of the Colombian hydrology through ENSO [*Shiff et al.*(1996)].

The purpose of this study is manifold, in particular: (i) to characterize the seasonal regional patterns of hydro-climatic anomalies in Colombia during El Niño and La Niña, (ii) to provide evidence of PS between the ENSO signal in the tropical Pacific Ocean and the annual and inter-annual variability of rainfall in the Colombia and, (iii) to investigate PS features between diverse macro-climatic processes and rainfall in Colombia during ENSO. This will allow improvements in diagnosis, understanding and management of water resources for socio-economical, environmental and ecological purposes in Colombia.

This work is organized as follows: section 3.3 presents the region of study; the hydro-climatic data sets are described in section 3.4, while the EEMD, GPD, SPS, and HyAns methods are presented in section 4.4. Finally, our results are discussed in section 4.5 and the conclusions are drawn in section 3.7.

3.3. Region of study

3.3.1. Natural regions of Colombia

As explained in Chapter 1, the continental territory of Colombia can be divided into five main natural regions (Fig. **3-1**) with different hydro-climatological, geomorphological and bio-ecological characteristics due to the influence of diverse geographical features and processes at different spatial and temporal scales.

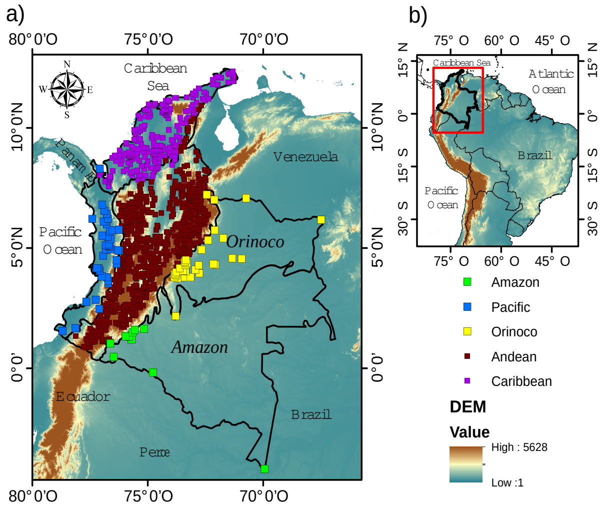

Figures 3-1.: Location of the region of study. (a) National context including the Colombian Natural Regions [IGAC, 2002] and rain gauges from IDEAM. (b) Continental context.

3.4. Data sets

3.4.1. SSTs in the tropical Pacific Ocean and the ENSO signal

We use the monthly Extended Reconstructed Sea Surface Temperatures (ERSSTv5) in the Niño 3.4 region (5^o N–5^o S and 170–120^o W) as well as Extreme Eastern Tropical Pacific SST or the Nino 1+2 zone (0^o–10^oS and 90^oW–80^oW). Details in https://www.cpc.ncep.noaa.gov. In addition, we use the monthly multivariate ENSO index (MEI) to classify the ENSO events, as explained in Chapter 2. Precipitation records were classified according to El Niño and La Niña months, as per the MEI definition. See details in Tables B-1 and B-2 (Suppl. Info.).

3.4.2. Colombian Precipitation datasets

*Dataset 1:*We use data from a reanalysis performed by [*Hurtado and Mesa*(2014)], which produced monthly precipitation fields for Colombia, spanning the period from 1975 to 2006, at a spatial resolution of 5 minutes of arc, in the region 5^oS–15^oN and 80^oW–65^oW. [*Hurtado and Mesa*(2014)] by using a set of 2270 rain gauges from diverse institutions including Instituto de Hidrología, Meteorología y Estudios Ambientales de Colombia (IDEAM), Empresas Públicas de Medellín (EPM), Centro Nacional de Investigaciones del Café (CENICAFE) and The Global Historical Climatology Network (GHCN). In addition, they also used satellite images from the Global Precipitation Climatology Project(GPCP)-V2, National Centers for Environmental Prediction (NCEP)/National Center for Atmospheric Research (NCAR), Tropical Rainfall Measuring Mission (TRMM), and the Geostationary Satellite System (GOES). Finally, the monthly precipitation fields resulted from a combination of the available data and the implementation of the PRISM model in the Colombian territory (see details in [*Hurtado and Mesa*(2014)]).

Dataset 2: We use a set of 937 rain gauges from IDEAM, at monthly timescale, having record lengths of 40 years, for the period 1976-2015, with less than 10% missing values. The geographical distribution of this data set is as follows: 38 time series for the Pacific, 631 in the Andean, 228 in the Caribbean, 30 in the Orinoco, and 10 in the Amazon region.

3.4.3. Other Macro-climatic Indices

We included further macro-climatic indices data, which are related to processes different from the ENSO system, namely: the `Tropical Northern Atlantic Index` (TNA), which consist of anomaly of the average of the monthly SST from 5.5^{o}N to 23.5^{o}N and 15^{o}W to 57.5^{o}W [*Enfield, et al.*(1999)], the `Tropical Southern Atlantic Index` (TSA) that contains the monthly average SST anomaly from Eq-20^{o}S and 10^{o}E-30^{o}W [*Enfield, et al.*(1999)], `North Atlantic Oscillation` (NAO) from NOAA Climate Prediction Center (CPC), available in https://www.cpc.ncep.noaa.gov. `Pacific Decadal Oscillation` (PDO), which is the leading PC of monthly SST anomalies in the North Pacific Ocean [*Zhang et al.*(1997),*Mantua*(2002)], `Atlantic multidecadal Oscillation` (AMO), which is calculated using is the Kalplan SST over the northern Atlantic, 0 to 70^{o}N [*Enfield, et al.*(2001)], and `Atlantic Meridional Mode` (AMM), which is defined via applying the Maximum Covariance Analysis to SST and the zonal and meridional components of the 10m wind field over the region (21^{o}S-32^{o}N, 74^{o}W-15^{o}E) [*Chiang and Vimont*(2004)].

These macro-climatic indices data were provided by NOAA Earth System Research Laboratory, freely available on https://www.esrl.noaa.gov/psd/data/climateindices/list/.

3.4.4. Reanalysis

We use data from the ERA5 atmospheric reanalysis [*Hersbach et al.*(2019)], which provides estimates of a large number of atmospheric, land and oceanic climate variables. The ERA5 data covers the Earth on a 30km grid and resolve the atmosphere using 137 levels from the surface up to a height of 80km. In particular, we use a spatial domain over Colombia (10^{o}S–20^{o}N and 85^{o}W–50^{o}W) for variables such as: monthly wind speed at pressure levels from 925hPa, vertically integrated moisture divergence, specific humidity, and vertical integrated water vapour fluxes (northward/eastward).

3.5. Methods

3.5.1. Generalized Phase Difference (GPD)

Theoretically, the GPD method was derived basing on physical properties of coupled oscillatory systems [*Rosenblum et al.*(2001)] (details in Appendix A). In practice, according to [*Pikovsky et al.*(2001)], the presence of a horizontal plateau in the phase difference vs. time diagram is the simplest way to evidence synchronization. In general, for two time series $x(t)$ and $y(t)$, their instantaneous phases $\phi_x(t)$ and $\phi_y(t)$, can be estimated using the analytic signal method expressed as [*Gabor*(1946), *Panter*(1965)],

$$Z_x(t) = x(t) + i\tilde{x}(t) = A_x^H e^{i\phi_x^H(t)} \tag{3-1}$$

where $\tilde{x}$ is the Hilbert transform (HT) of $x(t)$ defined as,

$$\tilde{x}(t) = \frac{1}{\pi}\text{p.v.}\int_{-\infty}^{\infty} \frac{x(t')}{t-t'}dt' \tag{3-2}$$

where p.v denotes the Cauchy's principal value.
From $Z_x(t)$ it is possible to calculate the instantaneous phase $\phi_x(t)$ as,

$$\phi_x^H(t) = \arctan\frac{Im(Z_x)}{Re(Z_x)}; \tag{3-3}$$

The instantaneous phase of $y(t)$, $\phi_y(t)$, can be calculated using a similar procedure. It is worth noting that HT is a non-parametric method and that the estimation of $\phi_x(t)$ and $\phi_y(t)$ based on the analytic signal (Eq. 3-1) is comparable with a technique based on wavelets [*Le Van Quyen et al.*(2001)].
Finally, denoting $\phi_x^H(t) = \phi_x$ and $\phi_y^H(t) = \phi_y$, the GPD can be expressed as,

$$\phi_{n,m} = n\phi_x - m\phi_y, \tag{3-4}$$

which in turn allows defining that $n : m$ *phase locking* appears if,

$$|\phi_{n,m} - s| < c, \tag{3-5}$$

where $c < 2\pi$ and s is the average phase between the two time series $x(t)$ and $y(t)$ [*Rosenblum et al.*(2001)]. However, for noisy oscillators or time series with oscillations at several frequency bands, the phase difference $\phi_{n,m}$ is unbounded due to phase jumps and the condition (Eq. 3-5) is not valid anymore. Nevertheless, the probability mass distribution of the *cyclic relative phase*

$$\Phi_{n,m} = \phi_{n,m}\texttt{mod}(2\pi) \tag{3-6}$$

has a dominating peak around a preferential value indicating phase synchronization in a statistical sense [*Rosenblum et al.*(2001)]. A stable phase locking in a ratio $n : m$ means n cycles of the oscillator x and m cycles of the oscillator y.
Hence, on the one hand, the GPD method has advantages such as: *(1)* the phase analysis allows, by means of $\phi_{n,m}$ plots, to trace transitions between qualitatively different regimes that are due to nonstationarity in the parameters of interacting systems and/or coupling and, *(2)* it is possible to apply this method even to very short records. On the other hand, the method has disadvantages such as: *(1)* the synchronous regimes of order different from $n : m$ shows nonsynchrony, *(2)* there are no straightforward methods to determine the integers n and m, so that they need to be identified by trial and error and, *(3)* if noise is relatively strong, this method becomes ineffective and may even be misleading [*Pikovsky et al.*(2001)].

3.5.2. Synchronization metrics

Strength of Phase Synchronization (SPS)

Although several *n:m synchronization indices* have been proposed in the literature (e.g. [*Rosenblum et al.*(2001)]), we use an index as measure of phase synchronization defined as,

$$\chi_t = \left| \left\langle e^{i(n\phi_x - m\phi_y)} \right\rangle_t \right| \tag{3-7}$$

The notation $\langle \cdot \rangle$ indicates temporal averaging. The index χ_t varies from 0 to 1, $\chi = 0$ indicates that the phases of the two time series are completely independent, while $\chi = 1$ indicates perfect phase synchronization [*Rosenblum et al.*(2001), *Stein et al.*(2014)].
In order to analyze the evolution of χ throughout the year, we calculate the long-term average of χ for each quarter.

3.5.3. Phase-Lag estimator

In classical time series analysis, the cross-correlation function is a well known linear technique to quantify the time-lag association between two time series. In phase synchronization analysis, lag synchronization occurs, when the phases of two interacting systems nearly coincide if one is shifted in time. To quantify the *lag*, we propose a function based on SPS as,

$$\chi(\tau) = \left| \left\langle e^{i\phi_{n,m}(\tau)} \right\rangle \right|, \tag{3-8}$$

where τ is the time-lag and $\phi_{n,m}(\tau)$ is the phase difference between the instantaneous phases $\phi_x(t-\tau)$ and $\phi_y(t)$, i.e. the GPD defined as $\phi_{n,m}(\tau) = n\phi_x(t-\tau) - m\phi_y(t)$, being x the ENSO signal and y a hydrological variable. The index $\chi(\tau)$ also varies from 0 to 1, with $\chi(\tau) = 0$ indicating non-synchronization and $\chi(\tau) = 1$ perfect phase synchronization.

3.5.4. Decomposition method

In the literature have been reported diverse techniques to decompose time series into its elementary patterns of behavior such as trends, oscillatory patterns, and noise [*Ghil et al.*(2001)]. In Chapter 2 was heightened the need for appropriate procedures of deseasonalization of time series. In such a work, the authors propose the F-filtering of the annual cycle (FAC) by moving averages (hereafter HyAns–FAC) as an adequate method to filter out the seasonal frequencies and their harmonics from the original climatic time series. Notwithstanding, the HyAns–FAC method allows decomposing a time series into two frequency bands: *(i)* noise, intra-annual and seasonal components and *(ii)* inter-annual frequencies. Here, we require a technique that allow us to decompose climate time series, at least, into three frequency bands: *(i)* seasonal components (or annual cycle), *(ii)* inter-annual variability, and *(iii)* intra-annual variability (high-frequency band) and noise. Hence, the EEMD method meets mentioned requirements and furthermore it has four similar properties to the HyAns–FAC method (see Chapter 2): *(i)* non-constant annual cycle, *(ii)* adequate separation of high and inter-annual frequencies, *(iii)* no-significant residual seasonal frequencies in anomalies and, *(iv)* the magnitude of extreme values of anomalies in a middle range compared with the other HyAns methods.
The EMD method has become a common and powerful tool in geophysical time series analysis [*Huang et al.*(1998), *Wu et al.*(2008), *Huang and Wu*(2008), *Wang et al.*(2015)]. EMD is useful to decompose non-linear and non-stationary time series into a set of Intrinsic Mode Functions (IMFs), which are extracted through an iterative, adaptive and temporally local procedure that does not force the data $x(t)$ to prescribed waves as traditional decomposition methods (e.i. sinusoidal waves or wavelets) [*Ghil et al.*(2001)]. However, the EMD method has a problem, it is not easy to associate physical variability modes to the IMFs because each IMF contains information in different frequency bands [*Wu et al.*(2008), *Rato et al.*(2008)]. To face up this "mode mixing" problem, [*Wu and Huang*(2005), *Wu and Huang*(2009)] proposed the EEMD allowing to decompose the original time series data, $x(t)$, into a set of IMFs exhibiting scale-consistent oscillation features. A brief summary of EMD and EEMD is presented in Appendix B.

3.5.5. Significance Tests

In this study, we apply two different statistical significance tests. The first significance test was proposed by [*Ahdesmäki, et al.*(2005)] as a robust method for detection of periodicities in time series. In our case, such a method allows us to guarantee that after decomposing of the hydrological time series into different frequency bands using EEMD: *(i)* the frequency band containing information at inter-annual timescales (hydro-climatic anomalies or HyAns) has no-significant seasonal residual and, *(ii)* the frequency band containing information at seasonal timescales (annual cycle) is adequately separated from the noise and inter-annual frequency bands. This procedure is necessary because the PS technique can be highly biased

by the presence of seasonal residual frequencies in anomalies (not shown here).
The second significance test is necessary to determine if the synchronization metrics are statistically significant. That means, we need to check if the strength of phase synchronization (see section 3.5.2) between X (the ENSO signal) and Y (the hydrological variable in Colombia) is a robust result. Hence, we develop a significance test for Phase Synchronization based on permutations, which is presented next.

Significance test for Phase Synchronization

Our study requires implementing a statistical test for the hypothesis of Phase Synchronization (PS) between the systems X and Y. In our case, X represents the ENSO system and $Y(\tau)$ denotes the hydro-climatic variables in Colombia, at defined time lags, τ. Then, we consider the original system X and a representative number of possible states of the system Y, which represent independent copies of the underlying system, so-called here synthetic time series (STS). For the construction of the STS from the system Y, we use permutations of the data points of the original time series Y but being careful to preserve the seasonality of the time series. That is, we permute data points in separate subsets for each month. e.g. we took all data points for January and put them randomly, after doing that for all months, we reconstruct a synthetic time series.
The null hypothesis is that each STS is an independent realization of the system Y, corresponding to a different initial condition or to a possible time series of the same system. To test the statistical significance of the strength of PS, $\chi(\tau)$, among X and $Y(\tau)$, we generate such 500 STSs of the Y system and obtain a test distribution of $\chi(\tau)$ calculated with the observations of the system X and each one of the STS of Y. Finally, we construct the upper 95% confidence interval (CI) based on the respective 95th percentile of the test distribution. The lags at which values fall outside the confidence band represent the ones where the null hypothesis is rejected, or that the system X is in PS with the system Y, i.e. they are phase dependent at that particular lag τ.

3.5.6. On the sensitivity of PS metrics in relation to diverse HyAns methods

Methods to estimate hydro-climatic anomalies (HyAns) have differences among them and therefore induce high-biases and error sources toward the interdependence analysis and modeling of climate time series. Moreover, such differences could generate ambiguities for the physical interpretation of results (see Chapter 2). Hence, we verify the sensitivity of PS metrics using the four HyAns methods assessed in Chapter 2, namely: *(i)* the Traditional Annual Cycle or constant climatology (HyAns–TAC), *(ii)* **F**-filtering of the Annual cycle by moving average (HyAns–FAC), *(iii)* Annual cycle extracted by Singular Spectrum Analysis or Singular-Spectrum Annual Cycle (HyAns–SSAC) and, *(iv)* the Modulated Annual Cycle or variable climatology, which is based on the EEMD technique. This PS analysis allows us to assess how sensitive or robust is our PS approach in relation to diverse methods to estimate HyAns.

3.5.7. PS between other Macro-climatic Indices and hydro-climatic anomalies in Colombia

Colombia's hydro-climatology can be influenced by processes that occur in other zones of the tropical Pacific Ocean (e.g. Nino 1+2) or low-frequency processes such as PDO. Likewise, Colombia's hydro-climatic variability is also influenced by macro-climatic processes that occur in the Atlantic Ocean, different from the ENSO system [*Poveda and Mesa*(1997), *Poveda et al.*(2001), *Poveda et al.*(2002), *Poveda et al.*(2004), *Poveda et al.*(2005), *Poveda et al.*(2011)]. Hence, we quantify PS using other macro-climatic indices such as TNA, TSA, NAO, AMO, AMM, and CAR. These cited works argue that such processes are related to hydro-climatic variability of Colombia, although such interdependence is still far from being understood in terms how the other macro-climatic processes influence anomalies over Colombia during ENSO. In this work, we quantify PS between HyAns in Colombia and other macro-climatic indices considering La Niña and El Niño epochs in order to shed light on non-linear spatio-temporal patterns of interdependence and their relationship with HyAns over Colombia.

3.6. Results and Discussion

3.6.1. PS between SST3.4 and rainfall in Colombia using raw data

We start analyzing phase relationships between SST in the tropical Pacific Ocean (ERSST3.4 containing its annual cycle) and the precipitation over Colombia (containing its annual cycle). The time series of precipitation are obtained by spatially averaging the monthly precipitation fields (Data set No. 1) separately for the five geographical regions of Colombia as shown in the Fig. **3-1**. With the purpose of comparing the original data, without extracting frequency bands, time series are standardized by subtracting the long-term average (grand-mean) and dividing by the long-term standard deviation (grand-standard deviation). Note that this standardization does not remove the annual cycle (AC).

Therefore, we use GPD and SPS to quantify PS between SST3.4 and precipitation over Colombia. Figure **3-2** (panel a) shows the time series of the MEI index and its periodogram (panel b) with different colors denoting the occurrence of El Niño and La Niña events during the period 1975-2006. In addition, Fig. **3-2** (panel c) shows the standardized time series and their periodograms (panel d) to visualize the spectral composition of both signals. Finally, Fig. **3-2** (panel e) evidence the presence of preferential values in the phase difference vs. time diagram, $\Phi_{1,1}(t)$, while Fig. **3-2** (panel f) evidences that the probability mass distribution

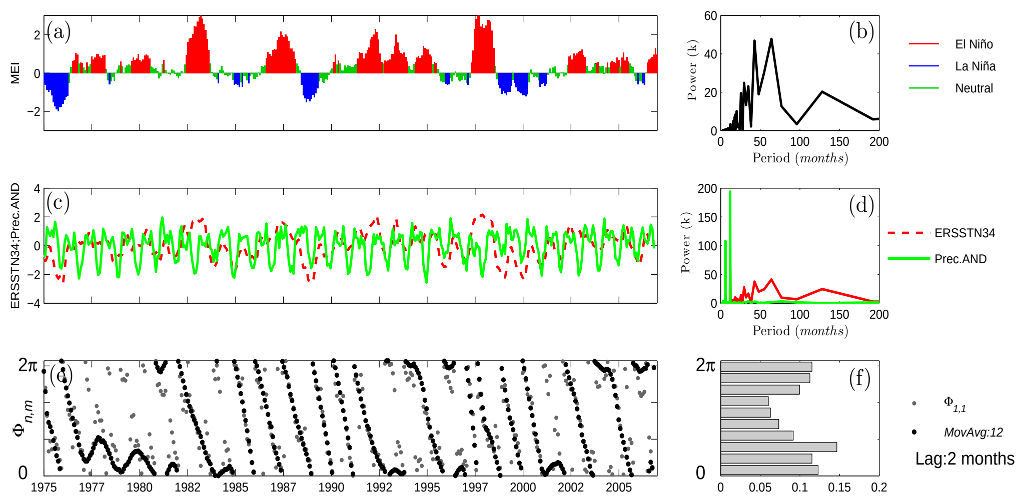

Figures 3-2.: Results of Phase difference $\Phi_{1,1}$ between SST3.4 (including its AC) and the long-term mean monthly precipitation (including its AC) for the Andean region of Colombia using the data set No. 1. (a) MEI index. (b) Periodogram of the MEI index (original time series). (c) Standardized time-series (without removing the annual cycle). (d) Periodograms of the time series. (e) Cylindrical representation of $\Phi_{1,1}$. (f) relative frequency distribution of $\Phi_{1,1}$.

of the cyclic relative phases has preferential values around $\Phi_{1,1} \sim 1.5\pi$ to 2π (September to February), indicating PS in a statistical sense, as we explained in section 3.5.1.

In general, Figure **3-3** shows the strength of PS, χ, between SST3.4 in the tropical Pacific and average precipitation for the five regions of Colombia, with a phase ratio 1:1 given that the predominant signal in both time series is the AC. Fig **3-3** (a-e) demonstrates χ as a function of time-lag $\tau = 1, 2, ..., 12$ months, where $\chi(\tau)$ is calculated using $\phi_{n,m}(\tau) = n\phi_x(t-\tau) - m\phi_y(t)$, being x the SST3.4 and y the precipitation time series (Details in 3.5.3). Our results evidence that PS is weak ($\chi < 0.40$) when the data are not classified according to the regimes of ENSO (El Niño and La Niña). In contrast, rainfall in the Pacific, Caribbean, Andean, and Orinoco regions exhibit stronger PS during La Niña than during El Niño. During La Niña, PS uncover a 2 months-lag, whereas during El Niño such time lag between the signals is not evident. Moreover, the Amazon region evidences a slightly stronger PS during La Niña than during El Niño, with 2 months-lag, which is not so clear as in the other regions. Figure **3-4** (Data set No. 1) shows the strength of PS, χ, as a moving-PS index between SST3.4 and average rainfall throughout each region (including their ACs). Our results evidence that the strongest El Niño events (1982-1983;1987-1988;1991-1992;1997-1998) exhibit weak PS, whereas La Niña events (1975-1976;1984-1985;1988-1989;1995-1996;1998-1999) exhibit strong PS. Analogous results were found for the rainfall dataset No. 2 (see the Suppl.

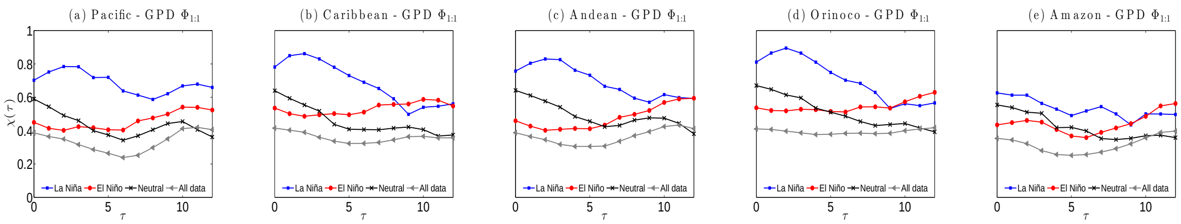

Figures 3-3.: Strength of phase synchronization, χ, between ERSST3.4 and long-term mean regional precipitation (both time series containing their annual cycles), using the Data set No. 1, with $\Phi_{1,1}$. (a-e) χ as a function of lag τ (in months) for El Niño and La Niña. (f-j) [right axis] χ for El Niño and La Niña with $\tau = 2$. [left axis] Average precipitation.

Info.). However, at this point, it is not possible to differentiate PS features between the El Niño events occurred in Eastern Pacific, Central Pacific or Mixed events, following the classification used by [Andreoli et al.(2017)].

Our analysis using raw data indicate three main results: *(i)* PS is weak, $\chi < 0.40$, when the data are not classified according to the states of ENSO (Niña and El Niño) for $\tau = 1, ..., 12$ months-lag, *(ii)* PS is strong during La Niña, $\chi \sim 0.80$, for $\tau = 2, ..., 4$ months-lag, exhibiting higher values for the Pacific, Caribbean, Andean, and, Orinoco regions, whereas the Amazon region exhibits moderate PS, $\chi \sim 0.60$, for $\tau = 1, 2$ months-lag, which suggest a lag-synchronization during La Niña, and *(iii)* during El Niño, the phase-lag function does not show a clear time-lag between the signals and there is no clear evidence of PS.

It is worth noticing that the PS results in Fig. **3-3** are calculated by spatially averaging of the monthly rainfall fields (Data set No. 1) for the five geographical regions of Colombia. Hence, the spatial averaging smooths the data and might hide slight phase differences among time series into the same natural region. Notwithstanding, we show clear differences in PS results regarding the states of ENSO although, at this point, it is hard to link such results with the annual cycle of rainfall in Colombia, the influence of ENSO on hydrological variables or the physical mechanisms behind PS. However, from our results discussed some remarkable questions arise:

- How significant is the ENSO signal in the original (raw) time series (which contain their annual cycles) regarding the states of ENSO (La Niña and El Niño)?
- Results indicate differences between data depending on whether they are classified by the states of ENSO. Is there PS between ENSO variability and rainfall anomalies over Colombia during all the ENSO states?
- Is there PS between the annual cycle of the hydrological variables in Colombia and the ENSO signal?

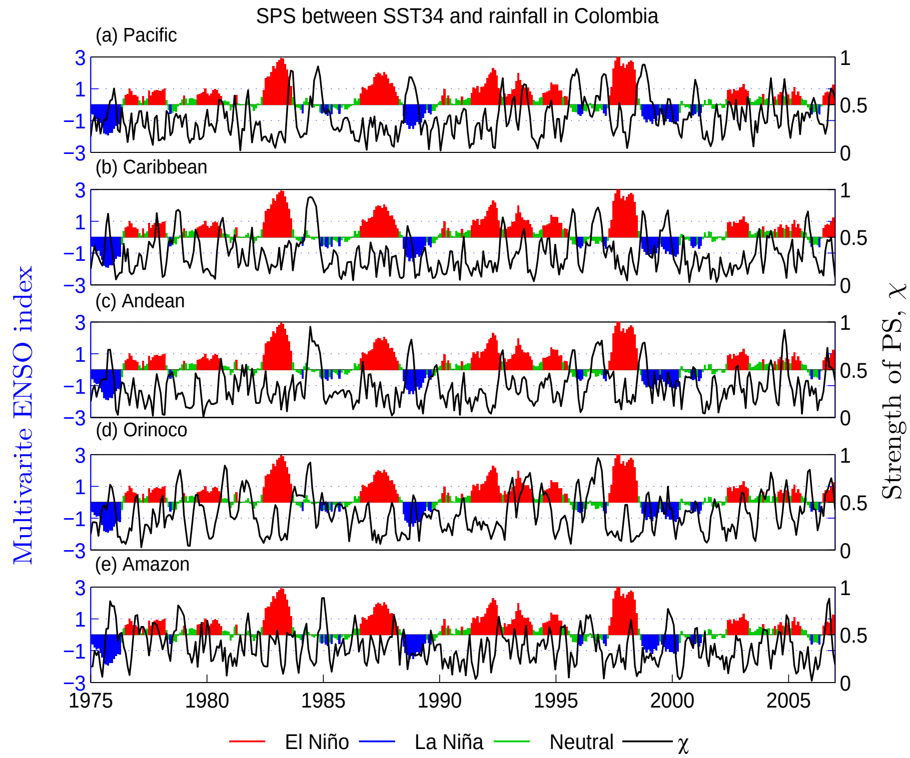

Figures 3-4.: Strength of phase synchronization between ERSST3.4 and long-term mean regional precipitation (both time series containing their annual cycles), using the Data set No. 1, with $\Phi_{1,1}$. [left axis] Multivariate ENSO index indicating periods El Niño, La Niña, and Neutral. [right axis] Strength of PS, χ.

- Is there any relationship between the Colombian zones that exhibit PS and the sign and magnitude of hydro-climatic anomalies?

In the next sections, we face up the above-mentioned questions and discuss our results in relation to physical mechanisms that control the annual cycle of rainfall and their anomalies during the warm and cold states of ENSO.

3.6.2. PS between SST3.4 and HyAns in Colombia at inter-annual timescales

Data pre-processing

In general, to quantify PS between the ENSO signal and the AC and HyAns in Colombia requires the following series of steps: *(i)* to define representative time series for the regions of Colombia, e.g. time series of rainfall or anomalies averaged over each natural region, *(ii)* to standardize the data (without subtract the seasonal variability), *(iii)* to filter out data in order to define the MAC, high-frequencies and noise of the hydro-climatic variables as well

Tables 3-1.: Percentage of the total variance, σ^2, explained by the MAC; Total Anomalies,A_T (in relation to MAC); Low-Frequency Anomalies, A_{LF}, and High-Frequency Anomalies,A_{HF}. Dataset No. 1.

Region	% σ^2 **MAC**	% σ^2 A_T	% σ^2 A_{HF}	% σ^2 A_{LF}
Andean	85.16	14.84	6.87	7.96
Caribbean	85.77	14.23	5.10	9.13
Pacific	72.63	27.37	16.27	11.10
Orinoco	92.66	7.34	1.59	5.74
Amazon	72.82	27.18	8.67	18.52

as their anomalies in relation to the MAC as explained by [*Wu et al.*(2008)], *(iv)* to test the significance of frequencies at seasonal timescales in the anomaly time series as stated by [*Ahdesmäki, et al.*(2005)] and, *(v)* to test the significance of the PS metrics (see section 3.5.5). The detailed steps behind our PS analysis are described in Suppl. Info (Section B.1).

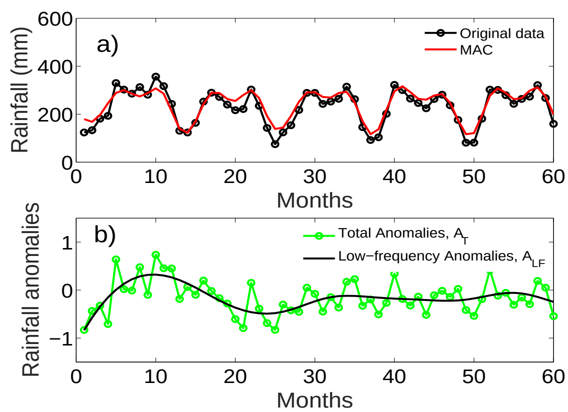

Figures 3-5.: Time series of rainfall and its standardized anomalies in the Andean region (Data set No. 1), example for a 5 years record length. a) Original averaged time series and its MAC. b) Rainfall anomalies after subtracting MAC or total anomalies, A_T and low-frequency anomalies or anomalies at inter-annual scales, A_{LF}.

Herein, we define high-frequency anomalies, A_{HF} as anomalies in frequency bands below 12 months, and low-frequency anomalies, A_{LF} that corresponds to anomalies in frequency bands above 12 months. In turn, the total anomalies A_T which are defined as the sum of A_{HF} and A_{LF}. Fig. **B-2** illustrates the difference between the original time series and MAC as well as the difference between A_T and A_{LF}. Furthermore, we verify the spectral characteristics of the original data, MAC, and A_{LF} for the time series of rainfall over each region (see Suppl. Info., Figs. B-1 to B-3)
In general, the MAC in relation to the total variance, σ_T, constitutes $\langle 82.0\% \rangle$ $[72.0\% - 93.0\%]$

and A_T constitutes $\langle 18.0\% \rangle$ $[7.3\% - 27.4\%]$. In turn, A_{HF} constitutes $\langle 8.0\% \rangle$ $[1.6\% - 16.3\%]$, whereas A_{LF} represents $\langle 10\% \rangle$ $[5.7\% - 18.5\%]$ (see details in Table **B-2**). Hereafter, we study the regional behavior of A_{LF} in Colombia and their association with ENSO.

Regional rainfall anomaly patterns

In Chapter 2 we show rainfall anomalies throughout Colombia considering the states of ENSO and using diverse methods to estimate hydro-climatic anomalies (HyAns). In general, Chapter 2 confirms that the Pacific, Andean and Caribbean regions exhibit negative (positive) rainfall anomalies during El Niño (La Niña) [*Poveda and Mesa*(1997), *Poveda et al.*(2001), *Poveda et al.*(2011), *Bedoya-Soto et. al.*(2018)]. Additionally, that work shows that Orinoco and Amazon regions exhibit positive (negative) rainfall anomalies during El Niño (La Niña). Hence, rainfall anomalies in the Pacific, Andean and Caribbean regions are opposite to those experienced in the Orinoco and Amazon regions during the warm and cold states of ENSO.

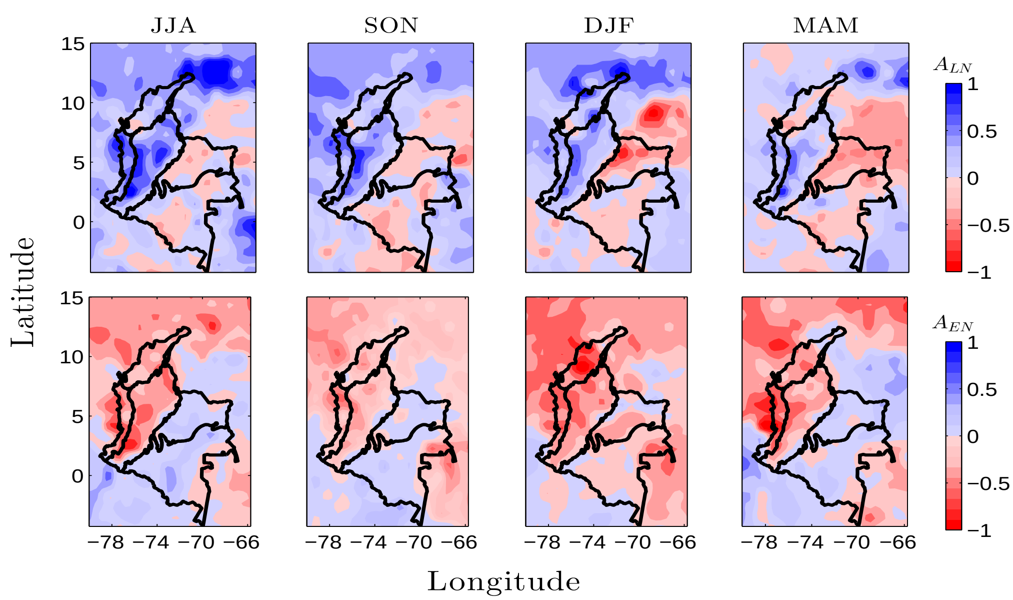

Figures 3-6.: Seasonal average composite rainfall anomalies (HyAns) over Colombia, during ENSO (Data set No. 1). (Top panels) HyAns during La Niña (A_{LN}). (Bottom panels) HyAns during El Niño (A_{EN}).

Here, we present the seasonal rainfall anomaly patterns in relation to ENSO. During La Niña, Fig. **3-6** (top row) evidences that the Pacific, Andean and Caribbean regions exhibit their highest positive rainfall anomalies during JJA and SON, whereas the Orinoco and Amazon regions exhibit their highest negative rainfall anomalies during DJF. During El Niño, Fig. **3-6** (bottom row) negative rainfall anomalies predominate throughout the year in the Pacific, Andean and Caribbean regions showing their maxima during DJF, which is the unique quarter where the complete continental territory of Colombia experiences negative rainfall anomalies. On the other hand, the Orinoco and Amazon regions exhibit positive rainfall anomalies during JJA, SON and MAM. Quarters that exhibit less impact by ENSO are MAM (SON) during La Niña (El Niño). Analogous results were found using the rainfall Data set No. 2 (see Fig. B-8 in Suppl. Info.).

During La Niña (El Niño), positive (negative) rainfall anomalies in the **Pacific** region can be explained in terms of the increasing (decreasing) moisture advection of the CHOCO jet as a result of increase (decrease) of the temperature gradient between surface air temperatures over the Pacific coast off Colombia and El Niño 1+2 zone during JJA and SON [*Poveda and Mesa*(2000), *Rueda and Poveda*(2006)]. Analogously, in the **Caribbean** region, positive (negative) rainfall anomalies could be explained through the influence of the CLLJ wind anomalies during ENSO. [*Wang*(2007)] and [*Martin and Schumacher*(2011)] showed that during JJA, rainfall in the Caribbean (including the Caribbean region of Colombia) exhibits significant correlations with the CLLJ index. Moreover, it is postulated that the CLLJ induces changes in moisture flux divergence in the Caribbean, which enhance convection and increase rainfall [*Martin and Schumacher*(2011)]. Furthermore, during La Niña, the easterly CLLJ winds are weak (strong) in JJA (DJF), whereas during El Niño, the easterly CLLJ winds are strong (weak) in JJA (DJF) [*Wang*(2007)]. [*Arias et al.*(2015)] mentioned that the weakening (strengthening) of the CLLJ winds is associated with increasing (decreasing) rainfall anomalies over northern Colombia. Hence, based on Gill's theory the weakening (strengthening) of the CLLJ winds is related to the increase (decrease) of the SST temperature in the Caribbean sea that subsequently increase (decrease) evaporation, increase (decrease) moisture convergence, and increase (decrease) rainfall in that zone [*Wang*(2007), *Martin and Schumacher*(2011), *Arias et al.*(2015)]. On the other hand, rainfall anomalies in the **Andean** region can be explained by the conjoint influence hydro-climatic processes of the Pacific and Caribbean regions, as well as by the land-surface atmosphere feedback, which manifest themselves in the fundamental role of local recycling moisture processes in the Magdalena and Cauca river basins [*Poveda et al.*(2014), *Arias et al.*(2015)]. In the **Orinoco** and **Amazon** regions, rainfall anomalies could obey to anomalies in the Orinoco LLJ which transport moisture from the Atlantic Ocean and subsequently, to induced-changes in local hydrological processes and terrestrial recycling from Amazon and Orinoco river basins [*Spracklen et al.*(2012), *Poveda et al.*(2014), *Arias et al.*(2015), *Hoyos et al.*(2017), *Jiménez-Sánchez*(2019)]. However, the dynamics of the Orinoco LLJ at interannual timescales and its influence on HyAns of the Orinoco and Amazon regions during ENSO constitutes an understudied topic, which is necessary to improve our knowledge on the HyAns of these regions under the ENSO influence. It is worth remarking that low-level jet anomalies are not the unique mechanisms influencing HyAns over Colombia but constitute an important mechanism of moisture transport and flux moisture divergence dynamics. Finally, HyAns in the Orinoco and Amazon also are influenced by the Cross-Equatorial winds [*Wang and Fu*(2002)] during ENSO, which also needs further research in order to advance in the understanding of HyAns of these regions.

3.6.3. Composites of hydro-climatic variables from ERA5 during ENSO

We carry out a composite analysis using ERA5 data, at a monthly resolution for the period 1979-2018, in order to verify the atmospheric conditions over northern South America and their relationships with rainfall anomalies over Colombia during the states of ENSO. In general, it is possible to confirm some aspects previously mentioned in section 3.6.2. During El Niño (La Niño) the SSTs over the far-eastern tropical Pacific are warmer (colder), Suppl. Info. Figures **B-9** and **B-10**, while surface winds are weaker (stronger) (see Fig. **3-7**).

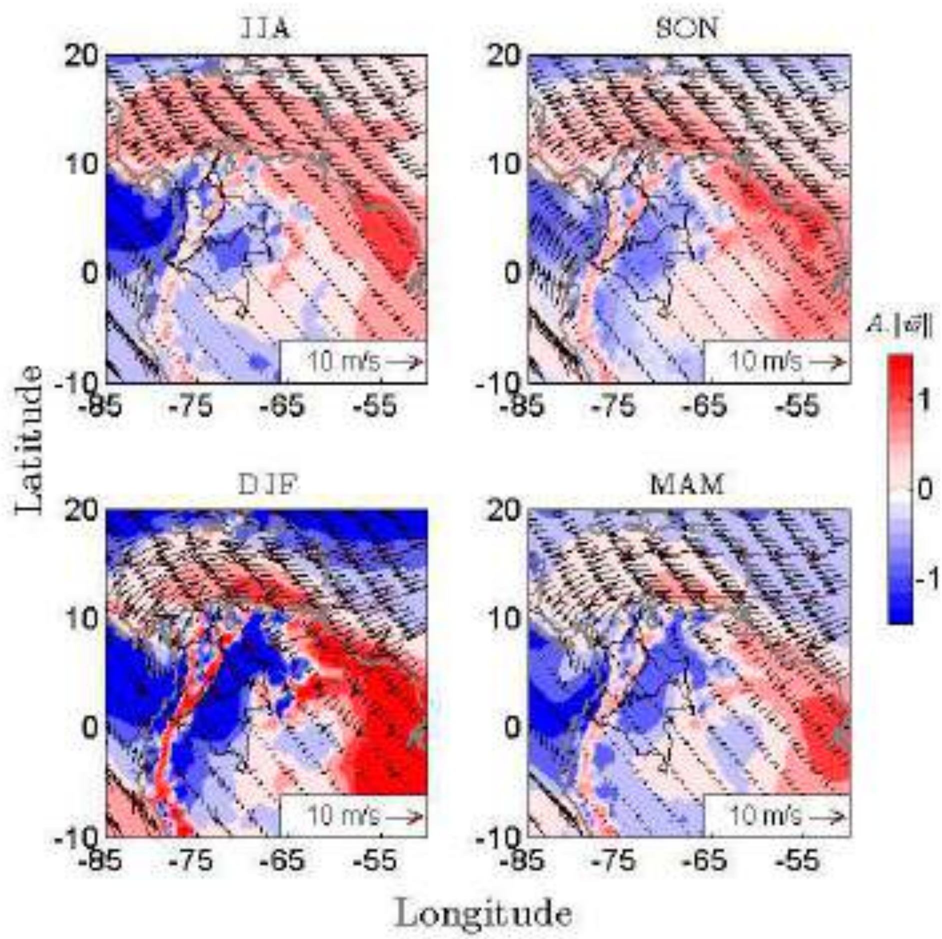

Figures 3-7.: Composite of anomalies of the surface winds magnitude at 100m ($A \cdot \|\overrightarrow{w}\|$) during El Niño. (arrows) climatology of winds during El Niño for the period 1979-2018 using ERA5.

Furthermore, during mentioned warm (cold) states of ENSO, the mean vertical integrated moisture divergences (mvimd) exhibit positive (negative) anomalies (see Fig. **3-8**), which coincide with negative (positive) rainfall anomalies over the Andean, Pacific, and Caribbean regions of Colombia as well as over the Caribbean sea (northern Colombia) as shown in Fig. **3-9**. During El Niño (La Niña), DJF (SON) experiences the highest negative (positive) rainfall anomalies.

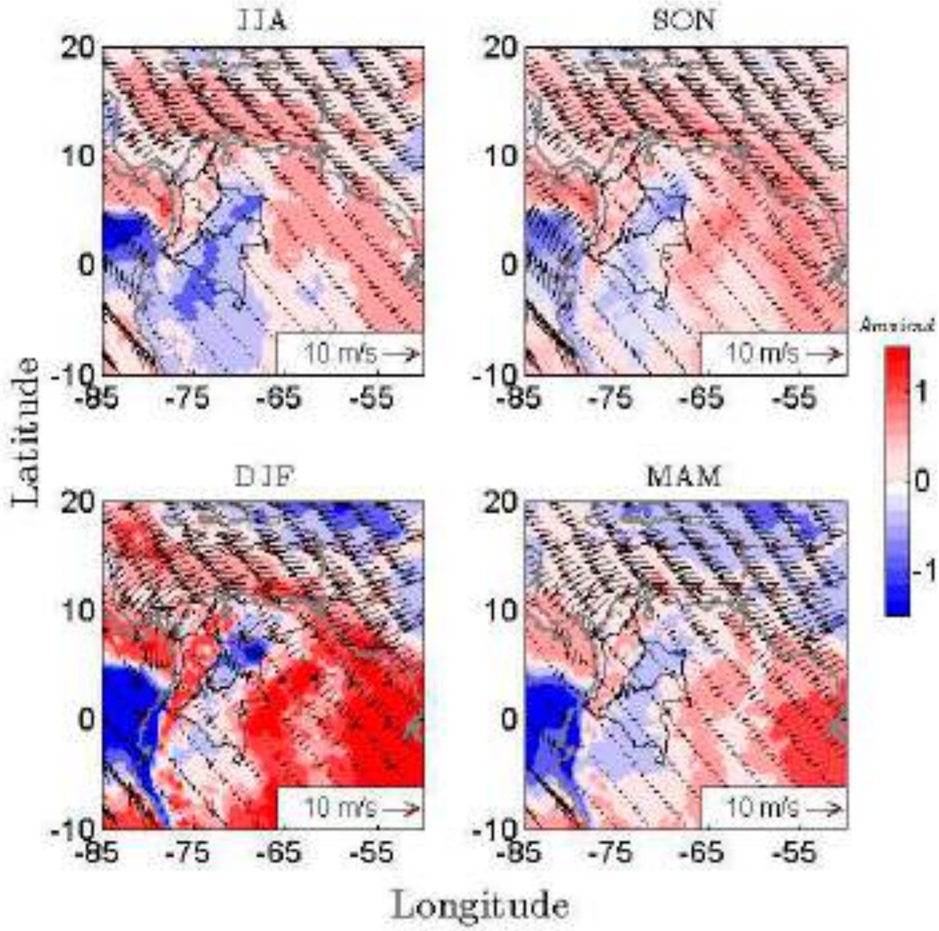

Figures 3-8.: Composite of mean vertical integrated moisture divergence (*Amvimd*) during El Niño. (arrows) climatology of winds during El Niño for the period 1979-2018 using ERA5.

Moreover, we analyze the volumetric soil water anomalies (VSW) during the states of ENSO. Our results evidence that during El Niño (La Niña), the VSW experiences negative (positive) anomalies. Those results confirm that ENSO impacts the soil water dynamics, which is a key component to advance in the understanding of land-atmosphere interactions over northern South America [*Cai et al.(2020)*, *Poveda and Mesa*(2000), *Bedoya-Soto and Poveda*(2017), *Bedoya-Soto et. al.*(2018), *Poveda et al.(2020)*].

Figures **3-7**, **3-8**, **3-9**, and **3-10** show only the results during El Niño. An analogous analysis was done for La Niña, which is can be seen in the Supp. Info. Figures **B-11**, **B-12**, **B-13**,

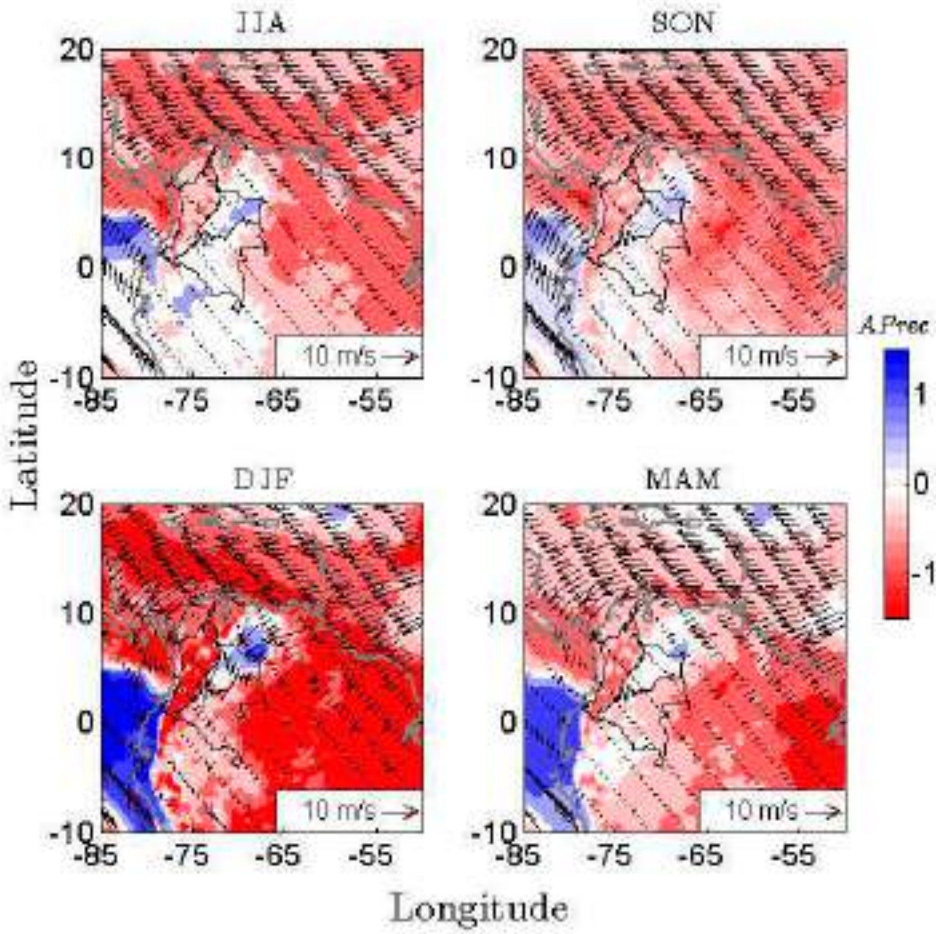

Figures 3-9.: Composite of rainfall anomalies ($APrec$) during El Niño. (arrows) climatology of winds during El Niño for the period 1979-2018 using ERA5.

and **B-14**.

PS between the ENSO signal and rainfall anomalies over Colombia

In this section, we quantify PS between SST3.4 anomalies and rainfall anomalies in Colombia. In addition, we calculate Pearson correlations between ENSO and HyAns in order to revise the ability of linear (Pearson) and non-linear techniques (PS) to capture spatio-temporal patterns of interdependence. This approach will allow us *(i)* reviewing possible physical mechanisms reported in the literature, (ii) comparing linear and non-linear quantifiers of interdependence, and *(iii)* hypothesize other possible processes that influence positive (negative) rainfall anomalies during La Niña (El Niño) in the regions of Colombia.
Fig. **3-11** (a-e) shows the strength of PS between SST3.4 anomalies in the tropical Pacific and rainfall anomalies in Colombia, as a function of time-lag τ, $\chi(\tau)$, using a phase ratio 1:1 (Data set No. 1). In this case, we use the time series of rainfall anomalies based on average

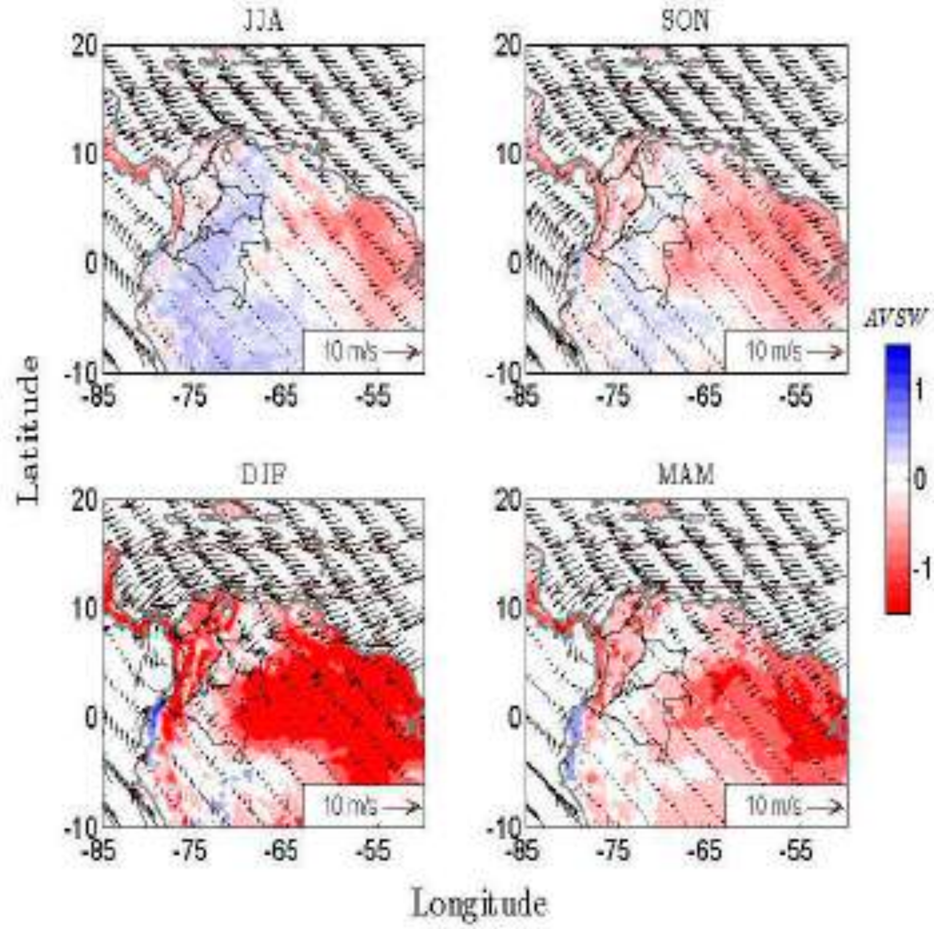

Figures 3-10.: Composite of volumetric soil water anomalies (AVSW) during El Niño. (arrows) climatology of winds during El Niño for the period 1979-2018 using ERA5.

rainfall over each Colombian region. Our results uncover strong PS (highly statistically significant) in the Pacific, Andean and Caribbean regions, whereas the Orinoco and Amazon regions do not exhibit clear PS (PS is not statistically significant). Furthermore, regions with significant values show stronger PS during La Niña than during El Niño. Moreover, during El Niño, we find lag-synchronization with 2-5 months-lag whereas during La Niña lag-synchronization is not evidenced. Similar results were found for the rainfall data set No. 2 (see Suppl. Info., Fig. B-15).

In addition, Fig. **3-12** shows the seasonal strength of PS, χ, between SST3.4 anomalies and HyAns in Colombia during the cold (top row) and warm (bottom row) ENSO's states. our results reveal that, during La Niña, the Pacific and Andean regions as well as a vast area over the Caribbean sea exhibit the strongest PS in JJA and SON, with geographic areas of significant PS that coincide with the seasons and localities of maximal positive rainfall

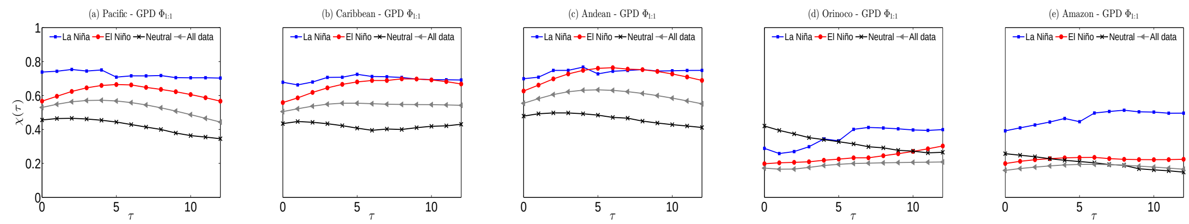

Figures 3-11.: Strength of phase synchronization, χ, between the SST3.4 anomalies and the standardized rainfall anomalies, A_{LF}. (Data set No. 1; 1976-2006) with $\Phi_{1,1}$. (a-e) χ as a function of lag τ (in months) during El Niño and La Niña for each region of Colombia.

anomalies. During El Niño, the Pacific, Caribbean, and Andean regions as well as the Caribbean sea show moderate PS, with the largest geographic area of significant PS during DJF, which coincide with the season and localities of maxim negative rainfall anomalies. The Orinoco and Amazon regions show non-significant PS during ENSO.

As a complement, Fig. **3-13** shows the seasonal Pearson correlations, r, between SST3.4 anomalies and HyAns during La Niña (top row) and El Niño (bottom row). Our results evidence that the r-values exhibit patterns of linear interdependence, which are not in agreement with the spatial patterns of seasonal rainfall anomalies over Colombia. To illustrate this, please see the spatial patterns of r during El Niño (Fig. **3-13**, bottom row) in relation to rainfall anomalies over Colombia (Fig. **3-6**, bottom row). It is worth to remark that, for the case of Colombia, the spatial patterns of Pearson correlation are highly sensitive to the method used to define Hyans in relation to the ENSO's states (see Chapter 2).

On the other hand, as explained in previous sections, the strength of PS, χ, exhibits high values when the phase differences, $\Phi_{n,m}$, between two time series have a dominating peak around a preferential value in the relative frequency distribution of $\Phi_{n,m}$. Then, only if $\chi_{n,m}$ has significant values it makes sense to interpret the mean value of $\Phi_{n,m}$, which can be understood as a time-lag between time series. Hence, Fig. **3-14** shows the average $\langle\Phi_{1,1}\rangle$ with overlapped hatched contours where $\langle\chi_{1,1}\rangle$ is statistically significant. In our case, a phase difference of $\frac{\pi}{3}$ approximates to 1 month lag. Then, Fig. **3-14** (top row) evidences that, at inter-annual time scales, during La Niña, for all quarters, SST3.4 anomalies in the tropical Pacific Ocean lead rainfall anomalies in the Pacific, Caribbean and Andean regions from 1 to 3 months lag. In contrast, during El Niño, JJA and SON, SST3.4 anomalies lead rainfall anomalies from 3 to 5 months lag. These results show that, during El Niño, rainfall anomalies exhibit a time-lag longer than during La Niña in relation to anomalies in the tropical Pacific ocean.

Summarizing, we found the following remarkable results: *(i)* strong (moderate) PS patterns in the Pacific, Caribbean and Andean regions were observed since the raw PS analysis (section 3.6.1, Fig. **3-3**), which was done using rainfall time series averaged over each

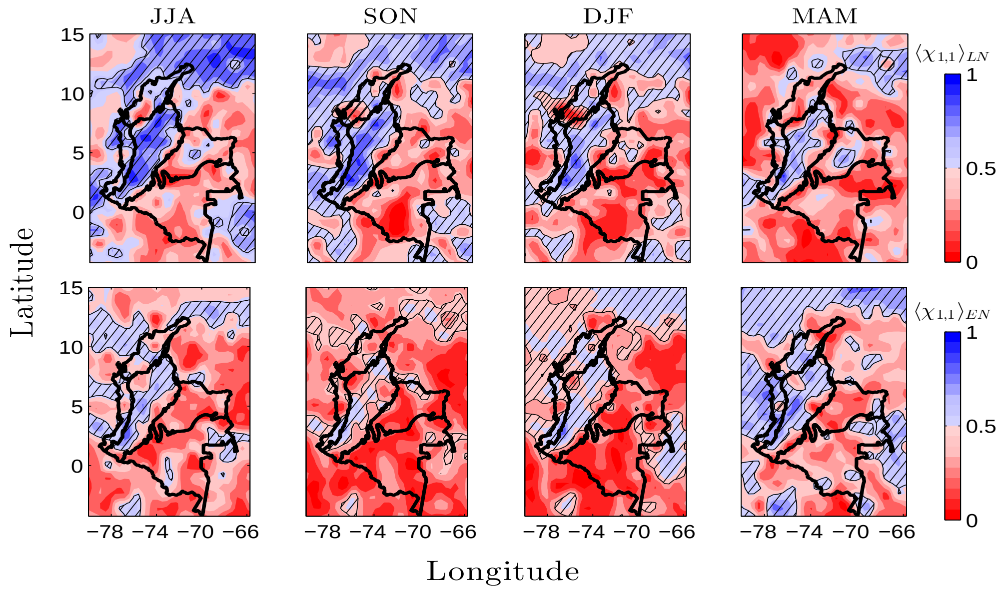

Figures 3-12.: Strength of phase synchronization between the standardized rainfall anomalies over Colombia (Data set No.1) and SST3.4 anomalies during ENSO. (top row) La Niña, $\langle\chi\rangle_{LN}$. (bottom row) El Niño, $\langle\chi\rangle_{EN}$. Phase ratio $\Phi_{1,1}$. The hatching contour lines indicate zones where χ is significant at 5%.

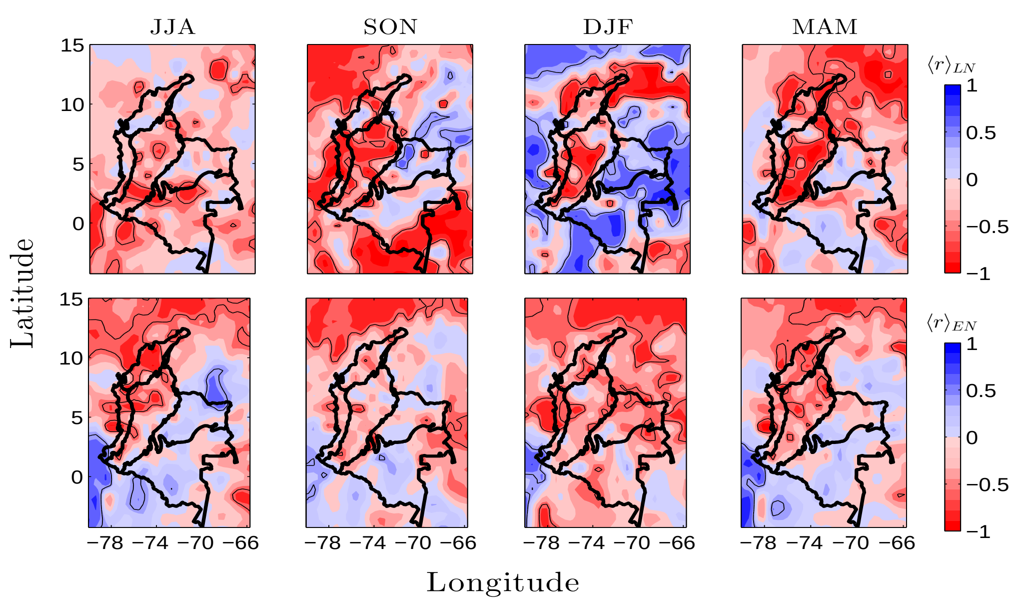

Figures 3-13.: Pearson correlations, r, between the standardized rainfall anomalies over Colombia and SST3.4 anomalies during ENSO. (top row) La Niña, $\langle r\rangle_{LN}$. (bottom row) El Niño, $\langle r\rangle_{EN}$. Contour lines denote zones where r is significant at 5%.

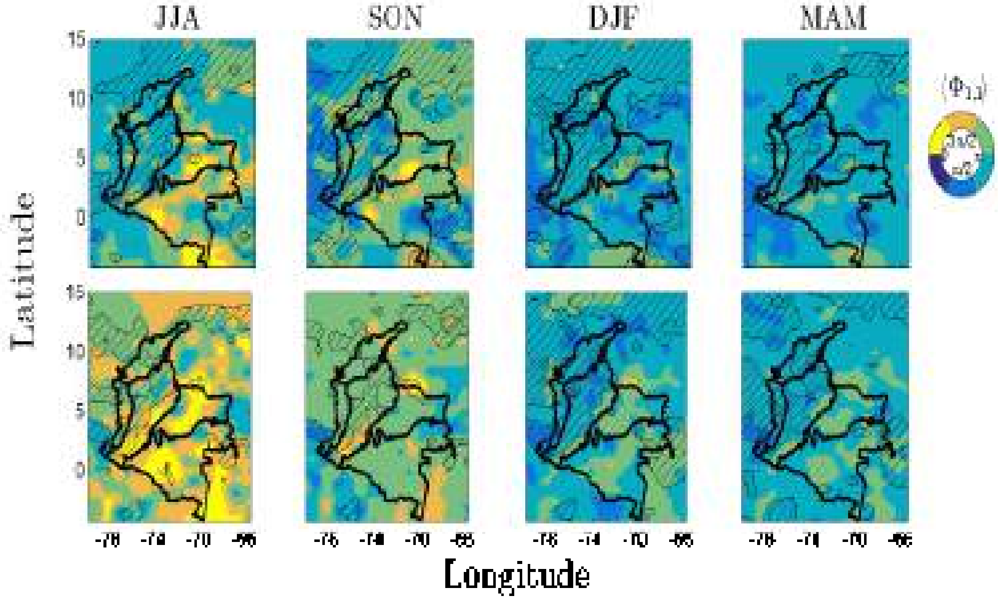

Figures 3-14.: Composite of average Phase Differences, $\langle\Phi_{1,1}\rangle$, between rainfall anomalies over Colombia and SST3.4 anomalies (Data set No. 1). (top row) La Niña. (bottom row) El Niño. A phase difference $\langle\Phi_{1,1}\rangle \approx \frac{\pi}{3}$ approximates to 1 month-lag. The hatched contours indicate zones where $\chi_{1,1}$ is significant at 5%.

region, *(ii)* the Generalized Phase Difference (GPD) technique helps to identify the spatial seasonal patterns of hydrological anomalies in Colombia in relation to the states of ENSO (La Niña and El Niño), whereas the linear Pearson correlation is not able to capture such patterns, and *(iii)* the Pacific, Andean and Caribbean regions are strongly (moderately) phase-locked with the tropical Pacific dynamics during La Niña (El Niño) in coherence with positive (negative) rainfall anomalies experienced in these regions. Hence, our PS results support the hypothesis of coupling between Colombian's climatology and the tropical Pacific Ocean dynamics in the mentioned regions, whereas the Orinoco and Amazon regions do not show PS with tropical Pacific Ocean variability. As discussed in section 3.6.2, PS results can be explained by a reduction (increase) of moisture advection from the CHOCO jet influencing the Pacific region [*Poveda and Mesa*(2000), *Rueda and Poveda*(2006), *Poveda et al.*(2014)] and by the strengthening (weakening) of CLLJ winds [*Wang*(2007)], which could inhibit (intensify) convection and rainfall in the Caribbean region [*Arias et al.*(2015)]. In the Andean region, the influence of the Caribbean and Pacific regions together with to the local hydrological processes enhanced by the large scale rivers basins and the orography of the Andean mountains helps to explain PS results associated to ENSO [*Poveda and Mesa*(1997), *Poveda et al.*(2001), *Poveda et al.*(2011), *Poveda et al.*(2014), *Arias et al.*(2015)]. Moreover, our results do not contradict the hypothesis that in the Orinoco and Amazon regions, the inter-annual dynamics of climate processes during ENSO are controlled by the

Atlantic Ocean dynamics [*Poveda et al.*(2014), *Arias et al.*(2015), *Hoyos et al.*(2017)].
Finally, our results uncover a link between the spatial PS patterns and rainfall anomalies during ENSO. Furthermore, it is well known that PS in non-linear oscillatory systems is defined as the appearance of a certain relation between the phases of interacting systems (or between the phase of a system and that of an external force), while the amplitudes can remain non-correlated [*Rosenblum et al.*(2001)]. On the other hand, generalized synchronization (GS) emerges when the state of the driven system is completely determined by the state of the driving system, i.e. the phases and amplitudes of both systems are correlated [*Pikovsky et al.*(2001)]. Hence, GS between ENSO and HyAns in Colombian regions that exhibit statistically significant PS is an open topic for further research.

Assessing PS between ENSO and rainfall anomalies in Colombia using diverse HyAns methods

We quantify PS using the four HyAns methods explained in Chapter 2, named: HyAns–TAC, HyAns–FAC, HyAns–SSAC, and HyAns–MAC (see section 3.5.6). The main objective is verifying how sensitive is the *Generalized Phase Difference* technique and the *Strength of Phase Synchronization* metric (hereafter PS metrics) in relation to diverse HyAns methods. To that end, we select the quarters that exhibit the strongest PS between SST3.4 and HyAns in Colombia, during La Niña and El Niño (i.e. JJA and DJF, respectively). Fig. **3-15** shows the PS in relation to the HyAns methods mentioned. Our results evidence that the strength of PS for the HyAns–FAC and HyAns–MAC methods are analogous, both methods exhibiting strong (moderate) PS during La Niña (El Niño) in JJA (DJF). PS metrics show similar results for HyAns–FAC and HyAns–MAC methods, for all quarters during La Niña and El Niño epochs. In contrast, PS metrics using the HyAns–TAC and HyAns–SSAC methods show significant differences with HyAns–FAC and HyAns–MAC. According to Chapter 2, HyAns–FAC and HyAns–MAC have some common properties, among them: *(i)* non-constant annual cycle, *(ii)* adequate separation of high and inter-annual frequencies, *(iii)* non-significant residual seasonal frequencies in anomalies and, *(iv)* the magnitude of extreme values of anomalies in a middle range compared with the other HyAns methods. On the other hand, HyAns–TAC and HyAns–SSAC do not meet the previously mentioned requirements for the case of rainfall anomalies over Colombia, which induce biases to results for quantification of interdependence by means linear and non-linear techniques.

3.6.4. PS analysis between ENSO and the AC of rainfall in Colombia

We quantify the strength of PS between the MEI signal (having only inter-annual frequency components) and the modulated annual cycle (MAC) of precipitation throughout Colombia. Fig. **3-16**a shows the MEI index and the states of ENSO (El Niño, La Niña, and Neutral). Fig. **3-16**b gives the cylindrical representation of the phase differences between the time series, $\Phi_{1,2}$. In this case, we do not classify data according to the states of ENSO then,

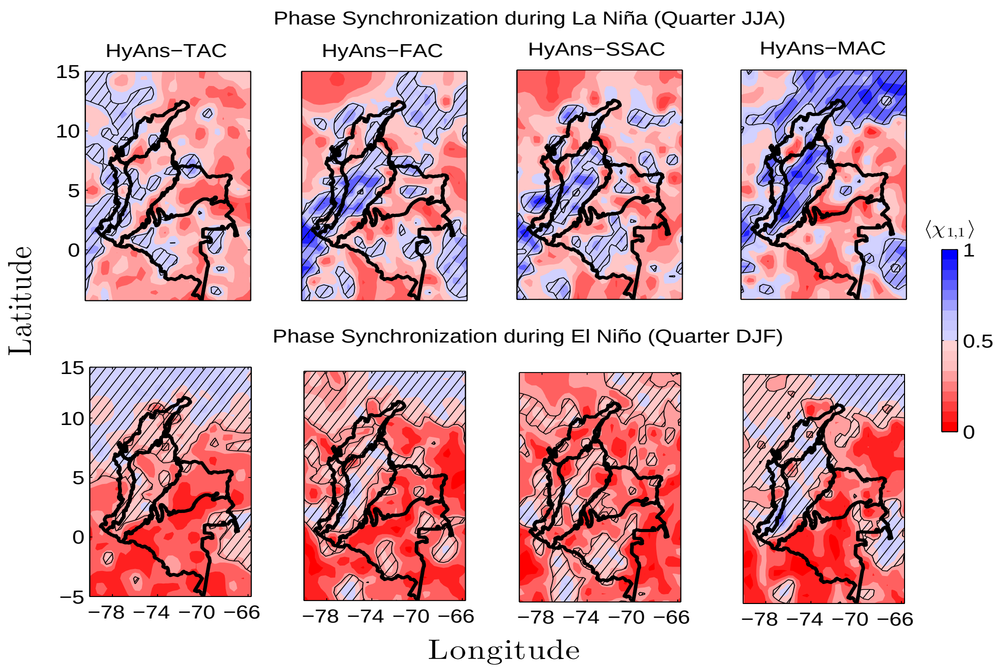

Figures 3-15.: Strength of Phase Synchronization, χ, between the SST3.4 anomalies and rainfall anomalies throughout Colombia, using the HyAns methods: HyAns–TAC, HyAns–FAC, HyAns–SSAC, HyAns–MAC for the quarters that exhibit the strongest PS during ENSO. Data set No. 1, period 1976-2006, phase ratio $\Phi_{1,1}$. (top row) χ for JJA during La Niña. (bottom row) χ for DJF during El Niño.

the almost uniform relative frequency distribution of $\Phi_{1,2}$ can be explained by the presence of data from the diverse states of ENSO. However, Figure **3-16** (panels c and d) evidences that the probability mass distribution of $\Phi_{1:2}$ is not perfectly phase-locked during El Niño (Fig. **3-16**c) and La Niña (Fig. **3-16**d) but certain phase differences are more probable than others. This behavior suggest some synchrony between the ENSO events and the AC of rainfall in Colombia.

Fig. **3-17**(a-e) shows the strength of PS between ENSO (SST3.4 anomalies) and the AC of rainfall throughout Colombia (Data set No. 1). We use as time series the monthly precipitation fields (and time series from rain gauges) spatially averaged over each region. Then, it is possible that such procedure smoothes the data and hides slight phase differences among time series. In general, PS is stronger during La Niña and El Niño than during the neutral ENSO's state. Furthermore, PS during El Niño is stronger than during La Niña. Moreover, our results suggest a non-lagged synchronization because the PS-function, $\chi(\tau)$, does not show prominent peaks for a specific time-lag $\tau \neq 0$. These results provide evidence that the inter-annual variability of ENSO is strongly phase-locked with the AC of rainfall over Colombia, particularly during El Niño and La Niña. Analogous results were found using the Data set No. 2 (not shown).

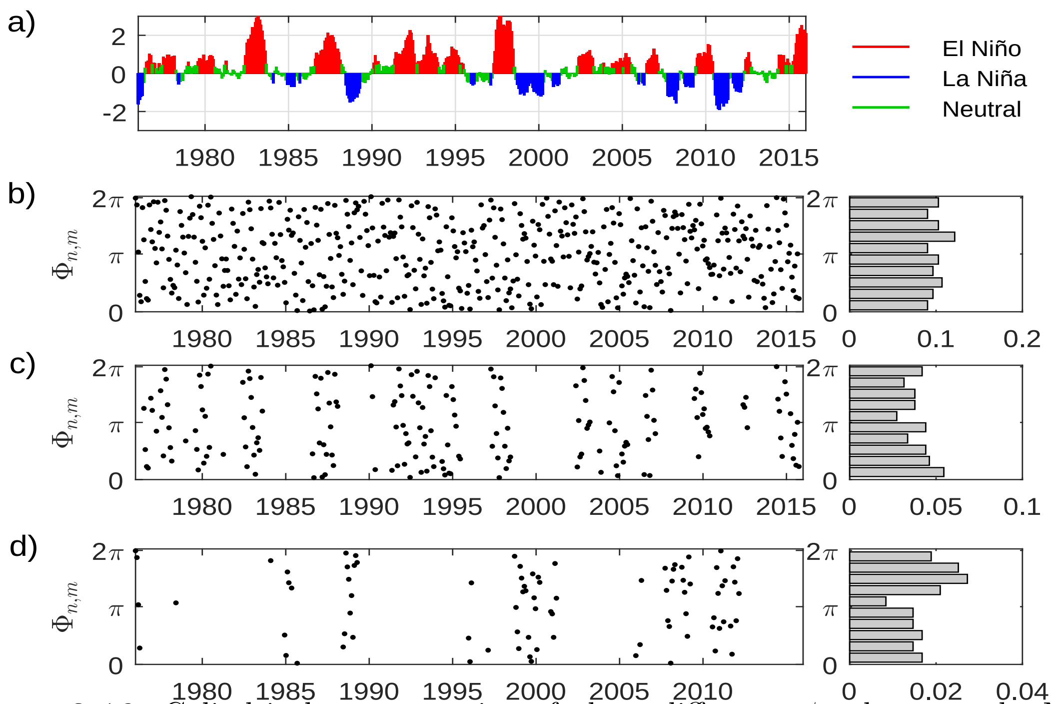

Figures 3-16.: Cylindrical representation of phase difference $\phi_{1,2}$ between the MEI index and the annual cycle of rainfall in the Andean region (Data set No. 2). (a) MEI index. (b) [left] $\phi_{1,2}$ using all record length data and [right] relative frequency distribution (c) [left] $\phi_{1,2}$ for El Niño state and [right] relative frequency distribution. (d)[left] $\phi_{1,2}$ for La Niña state and [right] relative frequency distribution.

Furthermore, we calculate the strength of PS, χ, between ENSO and the AC of rainfall using the two datasets available over Colombia in order to investigate spatial patterns of PS during La Niña and El Niño states. In general, Fig. **3-18** shows that in vast areas of the Colombian territory, the MAC of rainfall is strongly phase-locked with ENSO. Furthermore, the phase-locking patterns change depending on the season and the state of ENSO. **During La Niña**, Fig. **3-18** (top row) demonstrates strong PS, throughout the year, over the Caribbean sea, and the **Caribbean** and **Orinoco** regions. The northern **Andean** region exhibits significant PS during SON and DJF, whereas the southern Andean does not exhibit PS along the year. The central **Pacific** region exhibit PS in SON and DJF, while the Pacific region exhibit strong-PS during SON and the north Pacific coast of western Colombia shows strong-PS in DJF and MAM. Finally, a vast area in the **Amazon** region shows strong-PS during MAM and JJA. **During El Niño**, Fig. **3-18** (bottom row) shows strong PS in most of the Colombia territory along the year, except in southern Amazon and the south-western Colombian frontier with Ecuador in SON and DJF. During JJA a distinctive feature of non-PS crosses Colombian territory from the north-eastern Caribbean coast to the southern Pacific coast of Colombia (passing by the northern Andean region and the central Pacific

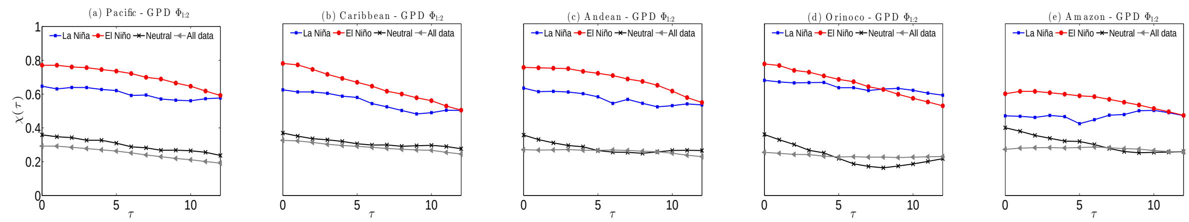

Figures 3-17.: Strength of phase synchronization, χ, between the SST3.4 anomalies and the MAC of rainfall throughout regions of Colombia (Data set No. 1; 1975-2006) with $\Phi_{1,2}$. (a-e) χ as a function of lag τ (in months) for El Niño and La Niña.

region). Further research is necessary in order to interpret these PS patterns in relation to the main mechanisms that determine the annual cycle of rainfall in such diverse regions.

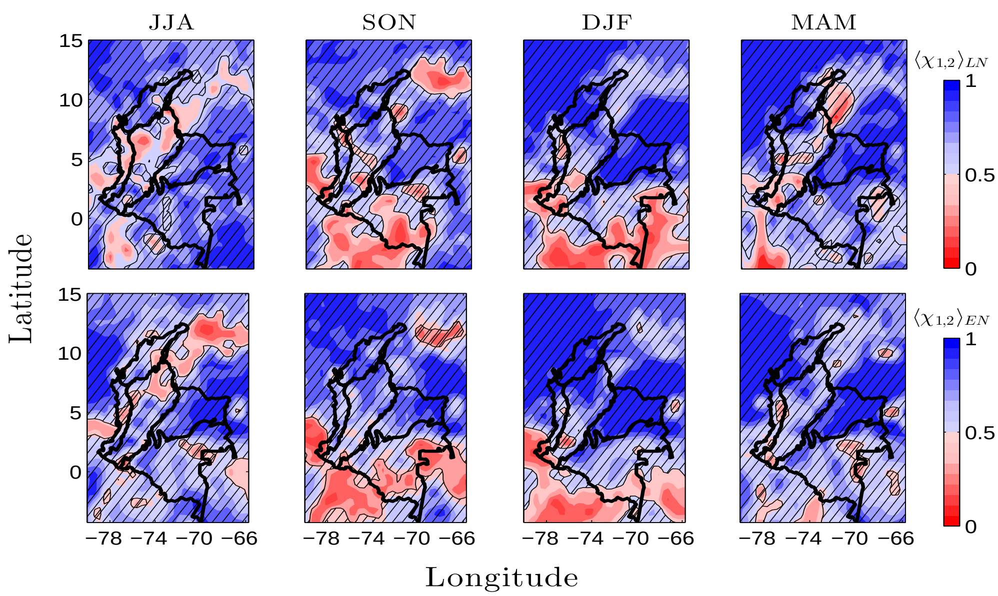

Figures 3-18.: Strength of phase synchronization, $\langle\chi\rangle$, between the SST3.4 anomalies and the modulated annual cycle (MAC) of precipitation over Colombia considering ENSO. Phase ratio $\Phi_{1,2}$, Data set No. 1. (top row) La Niña $\langle\chi\rangle_{LN}$. (bottom row) El Niño $\langle\chi\rangle_{EN}$. The hatched contours indicate zones where χ is significant at 5%.

As in section 3.6.3, the average Phase Differences, $\langle\Phi_{1,2}\rangle$, make sense only in areas where $\chi_{1,2}$ is statistically significant. Fig. **3-19** shows that although χ has similar strong-PS patterns between the ENSO signal and the AC of rainfall over most of the Colombian territory, the $\langle\Phi_{1,2}\rangle$ patterns change depending on the quarter and the ENSO state. During MAM and SON, when the ITCZ passes over central Colombia [*Hoyos et al.*(2017)], $\langle\Phi_{1,2}\rangle$ shows similar results for both La Niña and El Niño. In particular, $\langle\Phi_{1,2}\rangle$ exhibits a wave-like propagation

from the Orinoco region in direction to north and south, whose values are lower during MAM than during SON. In contrast, during La Niña and El Niño, in the boreal winter (DJF), when the ITCZ is located in its southernmost position [*Hoyos et al.*(2017)], $\langle \Phi_{1,2} \rangle$ exhibits a wave-like propagation, which increases from the Caribbean Sea to the central Orinoco region. Finally, during La Niña, in the boreal summer (JJA) when the ITCZ is located in its northernmost position, the phase differences are lower over the Caribbean Sea and higher over the northern Andean, Orinoco and Amazon regions. During El Niño, the $\langle \Phi_{1,2} \rangle$ values are higher over all Colombian territory than during La Niña.
In this sense, [*Stein et al.*(2014)] studied synchronization between ENSO and the annual cycle over the tropical Pacific Ocean. They investigated two possible mechanisms behind such synchronization feature, namely: (i) frequency locking of ENSO to periodic forcing by the annual cycle, or (ii) the effect of the seasonally varying background state of the equatorial Pacific on ENSO's coupled stability. As conclusions, their results indicated that the annual modulation of the coupled stability of the equatorial Pacific ocean-atmosphere system is by far the more likely mechanism generating the synchronization between ENSO and the annual cycle. In our case of study, at this point, PS between ENSO and the annual cycle of rainfall in Colombia cannot be associated with physical mechanisms behind the found PS patterns. However, the findings by [*Stein et al.*(2014)] allow us to hypothesize as a possible physical mechanism the annual modulation of the land-ocean-atmosphere interactions over northern tropical South America, which enhance or reduce the impact of ENSO on this regions. This hypothesis deserves further research.

3.6.5. PS between other macro-climatic indices and HyAns in Colombia

We quantify PS between rainfall anomalies throughout Colombia and other macro-climatic indices, such as: TNA, NAO, TSA, PDO, CAR, QBO, N12, AMO and AMM (see sections 3.4.3 and 3.5.7). To that end, we classify rainfall anomalies in Colombia and the macro-climatic time series, by considering La Niña and El Niño epochs as mentioned in Chapter 1. In addition, we filtered out the macro-climatic indices using EEMD in order to guarantee that time series preserve only the inter-annual frequency bands (see section B.1 and the Suppl. Info. B). Fig. **3-20** shows $\chi_{1,1}$ between the PDO index and rainfall anomalies in Colombia during ENSO (Data set No. 1). During La Niña in JJA, the PDO exhibits the strongest PS with rainfall anomalies over the Caribbean sea and the Caribbean, Andean, and Pacific regions. Furthermore, these regions coincide with zones of strong phase-locking between negative SST3.4 anomalies and rainfall anomalies (see Fig. **3-12** top row). Moreover, those areas of PS coincide with the Colombian regions that exhibit the highest positive rainfall anomalies (see Fig. **3-6** top row). During El Niño in JJA, SON, and MAM, the PDO also exhibits moderate PS with rainfall anomalies over the mentioned regions.
At this point, we hypothesize that some extreme positive (negative) anomalies over Colombia,

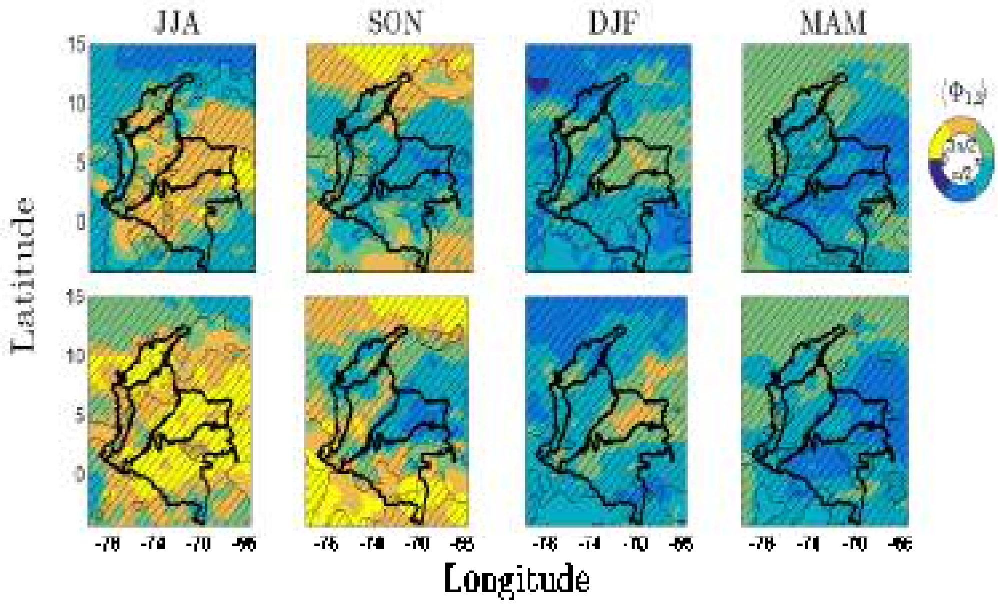

Figures 3-19.: Composite of the average Phase Differences, $\langle \Phi_{1,2} \rangle$, between SST3.4 anomalies and the MAC of rainfall over Colombia. (top row) La Niña. (bottom row) El Niño. The hatched contours indicate zones where $\chi_{1,2}$ is significant at 5%.

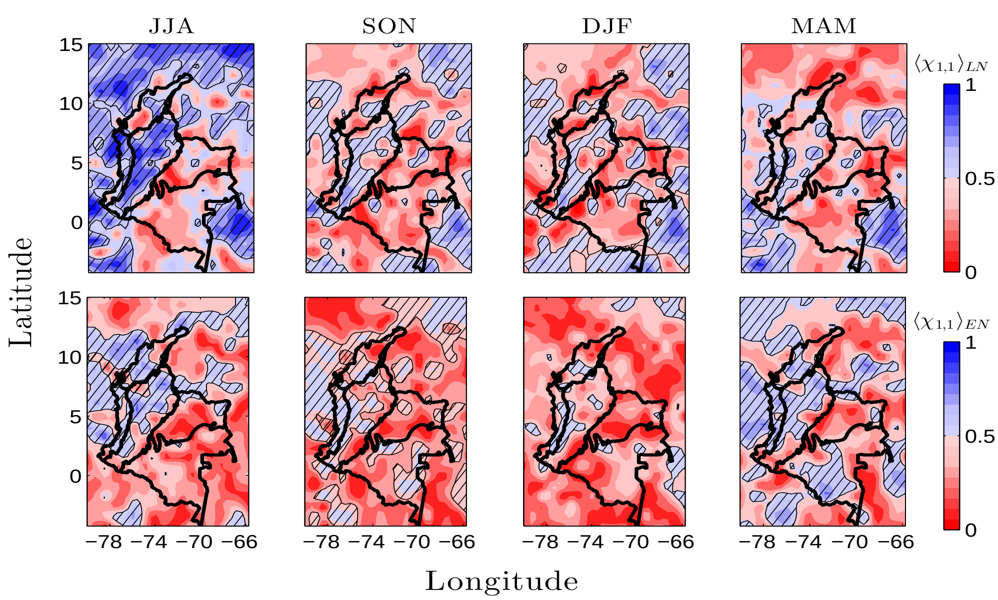

Figures 3-20.: Strength of phase synchronization, $\langle \chi \rangle$, between the PDO index and rainfall anomalies in Colombia during ENSO. Phase ratio $\Phi_{1,1}$, Data set No. 1. (top row) La Niña $\langle \chi \rangle_{LN}$. (bottom row) El Niño $\langle \chi \rangle_{EN}$. The hatched contours indicate zones where χ is significant at 5%.

during La Niña (El Niño), are enhanced by the conjoint effect of the PDO and the ENSO states. According to [*Mantua*(2001)], PDO primarily affects the North Pacific region but its effects can be felt also near the equator. Conversely, ENSO primarily affects the climate of lower latitudes, but its secondary effects are felt in the North Pacific. Furthermore, a positive (negative), or warm (cold) state of the PDO produces climate and circulation patterns that are similar to El Niño (La Niña) [*Gershunov and Barnett*(1998)]. Moreover, the climate signal of El Niño is likely to be stronger when the PDO is highly positive and conversely, the climate signal of La Niña will be stronger when the PDO is highly negative [*Gershunov and Barnett*(1998)].

To investigate our hypothesis, we quantify the strength of PS, χ, between the PDO index and SST3.4 anomalies as a moving PS-index using a 24-months window-length. In addition, we compare such moving PS-index with the rainfall anomalies averaged over each Colombian region in relation to the ENSO states according to the MEI index. For the **Pacific region**, Fig **3-21**a shows the MEI index and the ENSO states: La Niña, El Niño and Neutral. Fig **3-21**b gives the PDO index and the SST3.4 anomalies. Fig **3-21**c (right axis) shows the moving PS-index between PDO and SST3.4 anomalies whereas Fig **3-21**c (left axis) shows the rainfall anomalies. Note that during El Niño events (1982-1983, 1987-1988, and 1997-1998) the PDO-index exhibits positive values, while SST3.4 shows warm anomalies. At the same time, the moving PS-index exhibits weak PS, while Colombian Pacific rainfall experiments negative anomalies. Conversely, during La Niña events (1988-1989, 1998-1999, and 1999-2000) the PDO-index exhibits negative values while SST3.4 shows cold anomalies. At the same time, the moving PS-index shows strong PS while Colombian Pacific rainfall experiments positive anomalies.

Analogously, we quantify PS between rainfall anomalies in Colombia and NAO during ENSO (see Fig. **3-22**). Our results suggest that, during La Niña in JJA, NAO is strongly phase-locked with anomalies over the Andean and Caribbean regions. In this sense, [*Wang*(2007)] statedthat the Caribbean LLJ is phase-locked with the NAO. In addition, he argued that both the CLLJ and NAO are related to the NASH [*Wang*(2007)]. Hence, a strong (weak) NASH is associated with strengthening (weakening) of the easterly CLLJ and also corresponds to the positive (negative) phase of the NAO [*Wang*(2007)]. As a complement, the work by [*Arias et al.*(2015)] showed a significant linear correlation between the CLLJ and rainfall anomalies in Colombia. Neither [*Wang*(2007)] nor [*Arias et al.*(2015)] discussed differences of phase-locking and correlations in relation to the states of ENSO, which deserve future research. Notwithstanding, these results support the hypothesis that CLLJ wind anomalies during La Niña could contribute to explain positive rainfall anomalies over the Andean and Caribbean regions of Colombia.

Finally, the macro-climatic indices TNA, TSA, CAR, QBO, AMO, and AMM also exhibit areas of significant-PS with rainfall anomalies over Colombia (see Suppl. Info., Figs. B-17 and B-22). In particular, AMO is phase-locked with rainfall anomalies over the Amazon and Orinoco regions during El Niño and La Niña (see Suppl. Info., Fig. B-16). Also, TNA

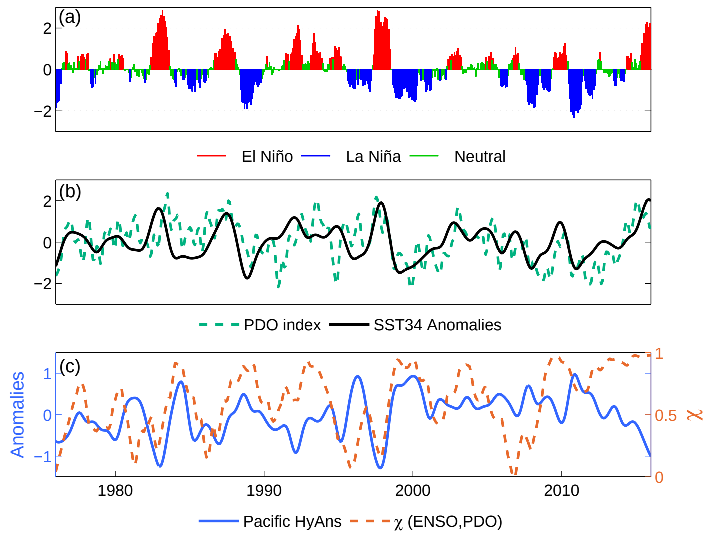

Figures 3-21.: Strength of phase synchronization, $\langle\chi\rangle$, between the PDO index and SST3.4 anomalies in relation to rainfall anomalies in the Pacific region of Colombia during ENSO. Phase ratio $\Phi_{1,1}$, Data set No. 2. (a) MEI index. (b) PDO index and SST3.4 anomalies. (c) Rainfall anomalies in the Pacific region of Colombia in relation to $\langle\chi\rangle$ between the PDO index and SST3.4 anomalies.

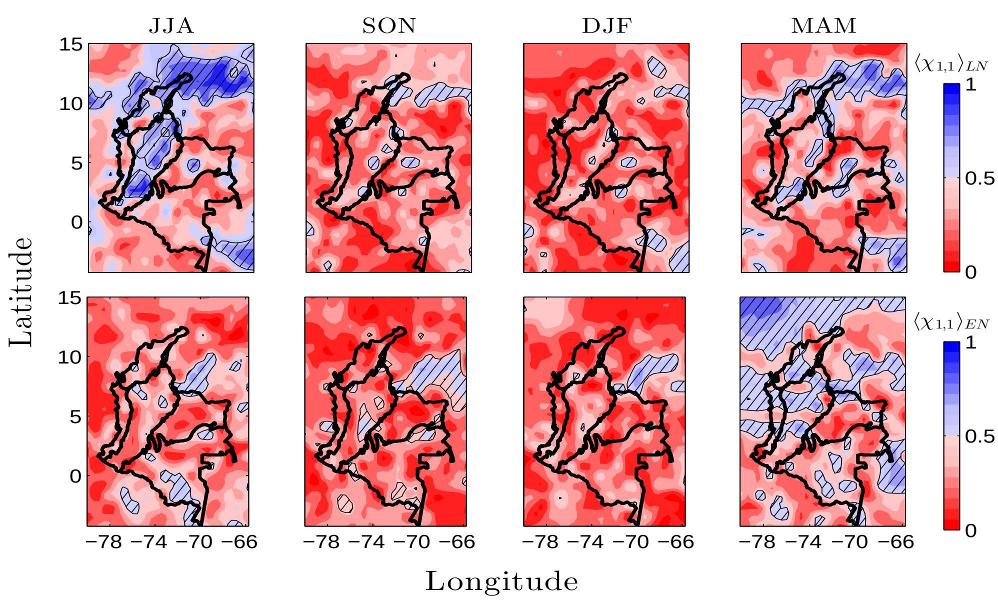

Figures 3-22.: Strength of phase synchronization, $\langle\chi\rangle$, between the NAO index and rainfall anomalies in Colombia during ENSO. Phase ratio $\Phi_{1,1}$, Data set No. 1. (top row) La Niña $\langle\chi\rangle_{LN}$. (bottom row) El Niño $\langle\chi\rangle_{EN}$. The hatched contours indicate zones where χ is significant at 5%.

shows phase-locking with rainfall anomalies over vast Colombian areas (see Suppl. Info., Fig. B-17). For the other macro-climatic indices, PS areas are smaller than those found for SST3.4 anomalies, the PDO and, the NAO signal. Furthermore, PS between HyAns and SST anomalies in the N12 zone as well as PS between HyAns and the MEI index provide similar results to those found for PS between HyAns and SST3.4 (see Suppl. Info., Figs. B-19).

3.7. Conclusions and future work

In this study, we have found five main results:
First, we present an unexplored approach based on Phase Synchronization (PS) techniques in order to investigate non-linear interactions between the ENSO signal in the tropical Pacific Ocean and the (annual and inter-annual) variability of rainfall over Colombia. To that end, we use the Generalized Phase Difference (GPD) technique as well as an index that provides a measure of the strength of PS. Our results show that the PS technique allows identifying seasonal spatial patterns of interdependence in relation to the extreme states of ENSO. However, for climate research purposes, the PS analysis must be accompanied by a rigorous data analysis in order to define adequately the annual cycle (AC), eliminate the seasonal residual frequencies in hydro-climatic anomalies, and assess the statistical significance of PS metrics. Moreover, we show that the PS technique is a robust method in relation to the different HyAns estimation methods, the HyAns-FAC and HyAns-MAC methods provide similar PS-results. This can be explained because the mentioned HyAns methods consider a non-constant annual cycle and it is possible to guarantee time series of anomalies with non-significant seasonal residual frequencies, which allow us avoid error sources and biases in quantification of PS.
Second, we study the seasonal regional rainfall anomaly patterns throughout Colombia during La Niña and El Niño. Our results evidence that, during La Niña (El Niño), the Pacific, Caribbean and Andean regions experiment positive (negative) rainfall anomalies, whereas the Orinoco and Amazon regions exhibit negative (positive) ones. During La Niña (El Niño), the Pacific, Caribbean, and Andean regions exhibit the highest positive (negative) anomalies in JJA (DJF) while the Orinoco and Amazon experiment the highest negative (positive) anomalies in DJF (JJA). Based on the literature, we discussed that such rainfall anomalies during ENSO can be explained by the influence of several concomitant hydro-climatic processes and mechanisms, among them: the three Low-Level jets surrounding Colombia (the Choco LLJ, the Caribbean LLJ, and the Orinoco LLJ), the Cross-Equatorial winds, land-surface atmosphere feedback (e.g. local recycling moisture in large river basins), other macro-climatic processes that are phase-locked with the ENSO signal (e.g. such as the PDO and the NAO), and the complex interactions between processes that occur at different timescales (e.g. ENSO signal in the tropical Pacific and the annual cycle of rainfall in Colombia). However, we also point out the need of further research on the LLJs anomalies and

the cross-equatorial wind anomalies during ENSO. Moreover, further research on the physical mechanisms behind the influence of other macro-climatic processes on hydro-climatic processes over Colombia is necessary.

Third, our findings reveal that the ENSO signal is strongly (moderately) phase-locked with rainfall anomalies over some Colombian regions during La Niña (El Niño). In particular, the PS analysis evidences that the significant seasonal spatial patterns of PS coincide with the seasonal spatial patterns of positive (negative) rainfall anomalies in the Pacific, Andean, and Caribbean regions during La Niña (El Niño). In the Orinoco and Amazon regions, rainfall anomalies do not exhibit significant PS with ENSO. Hence, our results support the hypothesis that rainfall anomalies in the Pacific, Andean and Caribbean regions are mainly influenced by the tropical Pacific Ocean dynamics, whereas rainfall anomalies in the Amazon and Orinoco regions are controlled by the Atlantic Ocean dynamics. Furthermore, we found that SST anomalies in the tropical Pacific ocean lead rainfall anomalies in Colombia with 3 to 5 months-lag during El Niño and 1 to 3 months-lag during La Niña. Moreover, the mentioned relationship between the PS patterns between ENSO and HyAns in Colombia point out the need of future research on the existence of Generalized Synchronization.

Fourth, we provide evidence of PS between the ENSO signal in the tropical Pacific Ocean and the modulated annual cycle (MAC) of rainfall over some regions of Colombia, which opens new paths towards the understanding of the non-linear feedback between the inter-annual variability of ENSO and the MAC of the hydro-climatic processes in Colombia. Although, at this point, it is not possible to provide a satisfactory physical explanation of such non-linear interdependence between ENSO and MAC. These results allow us hypothesizing as a possible physical mechanism, the annual modulation of the land-ocean-atmosphere interactions over northern tropical South America, which enhances or reduces the impact of ENSO on this regions. Future investigation on this topic is necessary.

Finally, we quantify PS between different macro-climatic indices and rainfall anomalies in Colombia. Our results reveal that the PDO signal and HyAns in Colombia are phase-locked. Such PS exhibits seasonal spatial patterns that are similar to those found for PS between the ENSO signal and HyAns over some regions. In this sense, we hypothesize that some extreme events of positive (negative) anomalies over Colombia, during La Niña (El Niño), are enhanced by the conjoint effect of the PDO and the ENSO states. Our analysis over the Pacific region of Colombia supports this hypothesis. In addition, we quantify PS between the NAO signal and HyAns in Colombia. In this sense, we found that during La Niña, in the boreal summer (JJA), HyAns in the Caribbean and Andean regions exhibit strong PS with NAO. Hence, a possible mechanism responsible for such phase-locking is the influence of the Caribbean LLJ winds anomalies on rainfall over the Caribbean and Andean regions of Colombia. In addition, we showed that other macro-climatic indices are phase-locked with rainfall anomalies, which suggest that several macro-climatic processes influence conjointly the hydro-climatology of Colombia. Moreover, such PS patterns from other macro-climatic indices also change depending on the ENSO's states.

3.8. Acknowledgments

The work of H.D. Salas is supported by COLCIENCIAS – Grant for National Doctorates 617-2 and partially funded by the Humboldt University of Berlin IRTG 1740. The work of G. Poveda and O. J. Mesa is supported by Universidad Nacional de Colombia at Medellin. The work by J. Kurths is supported by PIK. Thanks to: U.S. Geological Survey (USGS HydroSHEDS) for the Digital Elevation Models, NOAA for the ENSO index data, A. F. Hurtado for reanalysis data of precipitation over Colombia and, IDEAM the rain gauges records. Special thanks to J. M. Bedoya-Soto for the organized IDEAM dataset.

3.9. Appendix A:Phase Synchronization:Theoretical basis

According to [*Rosenblum et al.*(2001)], a stable limit cycle in the phase space is the main characteristic of stable periodic self-sustained oscillators. Then, the dynamics of a phase point on this cycle can be denoted as,

$$\frac{d\phi}{dt} = \omega_o \tag{3-9}$$

where $\omega_o = 2\pi/T_o$, and T_o is the period of the oscillation. On the other hand, if two oscillators are weakly coupled, it is possible to neglect variations of amplitudes to obtain equations describing their phase dynamics such as,

$$\frac{d\phi_1}{dt} = \omega_1 + \epsilon g_1(\phi_1, \phi_2) \; ; \quad \frac{d\phi_2}{dt} = \omega_2 + \epsilon g_2(\phi_2, \phi_1) \tag{3-10}$$

where the coupling terms g_1 and g_2 are 2π-periodic in both arguments, and ϵ is the coupling coefficient.
Hence, as the interaction between the oscillators essentially effects the evolution of their phases if the frequencies ω_1 and ω_2 are in resonance, i.e. if for some integers n and m, $n\omega_1 = m\omega_2$ [*Rosenblum et al.*(2001)].
Then, in the first approximation, the Fourier expansion of the functions g_1 and g_2 contains slowly varying terms $\sim n\phi_1 - m\phi_2$ and under such assumption the *generalized phase difference* can be defined as,

$$\Phi_{n,m}(t) = n\phi_1(t) - m\phi_2(t), \tag{3-11}$$

Subtracting Eq.(3-10) and keeping only the resonance terms, we get

$$\frac{d\Phi_{n,m}}{dt} = n\omega_1 - m\omega_2 + \epsilon G(\Phi_{n,m}) \tag{3-12}$$

where $G(\cdot)$ is 2π-periodic. In addition, Eq. (3-12) is a one-dimensional ordinary differential equation that admits two types of solutions: fixed points or periodic rotations of $\Phi_{n,m}$. The

stable fixed point corresponds to perfect phase locking, when $\Phi_{n,m} = const.$ The periodic rotations describe quasi-periodic motion with two incommensurate frequencies in the system presented in Eq. (3-10) [*Rosenblum et al.*(2001)].
Finally, considering a small coupling in the Eq. (3-10), it is possible neglect the non-resonant terms. With non-resonant terms, the condition of synchronization of periodic oscillators should be generally written as a phase locking condition,

$$|n\phi_1(t) - m\phi_2(t) - \delta| = const., \tag{3-13}$$

where δ is some (average) phase shift, or as a frequency entrainment condition,

$$n\Omega_1 = m\Omega_2, \tag{3-14}$$

where

$$\Omega_{1,2} \approx \left\langle \frac{d\phi_{1,2}}{dt} \right\rangle \tag{3-15}$$

It is worth mentioning that in the synchronized state the phase difference is generally not constant but oscillates around δ.

3.10. Appendix B: Decomposition methods based on EMD

3.10.1. Empirical Mode Decomposition (EMD)

[*Huang et al.*(1998), *Huang et al.*(1999)] proposed that a time series, $x(t)$, can be expressed as,

$$x(t) = \sum_{j}^{n} (c_j(t)) + \zeta \tag{3-16}$$

where c_j correspond to the IMFs, and ζ the residual of data. The procedure can be summarized as follows [*Huang et al.*(1998)]: (1) The extreme maximum and minimum values are identified in $x(t)$, (2) the maximal values are connected using a cubic spline to find an upper envelope, $U_{max}(t)$. A similar procedure is carried out to the minimal values to find a lower envelope, $L_{min}(t)$, (3) the mean value between $U_{max}(t)$ and $L_{min}(t)$ is estimated [$\bar{U}(t) = \frac{U_{max}(t) - L_{min}(t)}{2}$], (4) the time series $\bar{U}$ is substrated of $x(t)$ [$d(t) = x(t) - \bar{U}(t)$], (5) the time series $d(t)$ is considered as the new $x(t)$ and then steps 1–4 are repeated until finding a signal with zero mean that is the first IMF, (6) The IMF is subtracted from the original time series $x(t)$ and the procedure is repeated to obtain the next IMF, and (7) stop the iterative process when $d(t)$ has only one maximum or one minimum value, so that it is not possible to extract more IMFs using $d(t)$.

3.10.2. Ensemble EMD (EEMD)

As mentioned above, [*Wu and Huang*(2005), *Wu and Huang*(2009)] proposed the EEMD as a modified version of the EMD method to solve the "mode mixing" problem. The procedure can be summarized as follows: (1) add white noise series to the original data $x(t)$, (2) apply the EMD method to $x(t)$ with added noise to find the IMFs, (3) repeat steps (1) and (2) several times and, (4) calculate the (ensemble) mean for each IMF, until finding stable values of the IMF for a given error level ϵ.

Finally, the added noise series cancel out each other and the mean IMFs remains within the natural dyadic filter windows significantly reducing the chance of mode mixing and preserving the dyadic property [*Flandrin et al.*(2004), *Wu and Huang*(2005), *Wu and Huang*(2009), *Wu et al.*(2008)]. This method is counter-intuitive because it uses multiple noise realizations added to a single time series to mimic a scenario of multiple trials of observations which are averaged for the corresponding IMFs allowing to extract scale-consistent signals [*Wu et al.*(2008)].